Measurement report: VOC characteristics at the different land-use types in Shanghai: spatio-temporal variation, source apportionment, and impact on secondary formations of ozone and aerosol

Yu Han[1], Tao Wang[1], Rui Li[1], Yang Li[1], Hongbo Fu*[1, 2, 3], Yusen Duan[4], Song Gao[4, 5], Liwu Zhang[1], Jianmin Chen[1, 2]

[1]Shanghai Key Laboratory of Atmospheric Particle Pollution and Prevention, Department of Environmental Science & Engineering, Fudan University, Shanghai, 200433, P.R. China; [2]Institute of Eco-Chongming (SIEC), 20 Cuiniao Road, Chenjia Town, Chongming District, Shanghai 202162, China; [3]Collaborative Innovation Center of Atmospheric Environment and Equipment Technology (CICAEET), Nanjing University of Information Science and Technology, Nanjing 210044, P.R. China; [4]Shanghai Environmental Monitoring Center, National Environmental Protection Shanghai Dianshan Lake Science Observatory Research Station, Shanghai, 200235, China; [5]School of Environmental and Chemical Engineering, Shanghai University, Shanghai, 200444, China

Correspondence to: Hongbo Fu (fuhb@fudan.edu.cn)

Abstract. Volatile organic compounds (VOCs) have important impacts on air quality, climate change and human health. In order to identify the spatio-temporal variations, sources and ozone (O_3) and secondary organic aerosol (SOA) formation potentials of the atmospheric VOCs, a concurrent multi-site observation campaign was performed at the supersites of Shanghai, East China, in the first three months of 2019. The sampling sites are located at the different land-use types including industrial district (the Jinshan site: JS), residential and commercial mixed districts (the Pudong site: PD) and background district (the Qingpu site: QP) of Shanghai. During the observation period, the average VOC concentrations were sensitive to the land-use types in the order of JS (21.88 ± 12.58 ppb) > PD (21.36 ± 8.58 ppb) > QP (11.93 ± 6.33 ppb) sites. The predominant VOC category was alkanes (49.32-71.48 %), followed by aromatics (10.70-21.00 %), alkenes (10.13-15.30 %) and alkyne (7.69-14.80 %) at the studied sites. There were distinct diurnal variations and "weekend effects" of VOCs at the sampling sites. The VOC concentrations increased by 27.15, 32.85 and 22.42 % during the haze events relative to the clean days. Vehicle exhaust was determined as the predominant VOC source. The second largest VOC contributor was identified as industrial production at the JS and PD sites, while it proved to be fuel production and evaporation at the QP site. The industrial emission and biomass burning showed slight contributions to VOC concentrations at the QP and JS/PD sites, respectively. It was consistent with the regional characteristics of anthrogopenic activities dominated by land-use types. High potential source contribution function (PSCF) values primarily appeared in the northeastern and northern areas surrounding sampling sites, suggesting the strong local emissions. The ozone formation potentials (OFP) values of each land-use types were in order of JS (50.89 ± 2.63 ppb) > PD (33.94 ± 1.52 ppb) > QP (24.26 ± 1.43 ppb) sites, with alkenes and aromatics being the predominate contributors. Secondary organic aerosol formation potential (SOAFP), mainly contributed by the aromatics, was the highest at the JS site (1.00 ± 2.03 μg m^{-3}), followed by the PD (0.46 ± 0.88 μg m^{-3}) and QP (0.41 ± 0.58 μg m^{-3}) sites. The VOCs-PM$_{2.5}$ sensitivity analysis showed that VOCs at the QP

site displayed a more rapid increment along with the increase of PM$_{2.5}$ values relative to the other two sites. Alkenes and aromatics are both the key concerns in controlling the VOC-related pollution of O$_3$ and SOA in Shanghai. These findings provide more information on the accurate air-quality control at a city level in China. The results shown herein highlight that the simultaneous multiple-site measurements with the different land-use type in the megacity or city cluster could be more appropriate to fully understand the VOC characteristics relative to a single-site measurement performed normally.

1. Introduction

Serious air pollution in China is currently characterized by the high levels of ozone (O$_3$) and fine particulate matters (PM) especially PM$_{2.5}$ (PM with an aerodynamic diameter less than 2.5 μm). The atmospheric volatile organic compounds (VOCs) greatly influence the O$_3$ and PM$_{2.5}$ formations, and function as the important precursors (Carter, 1994; Liu et al., 2008; Yuan et al., 2013; Lu et al., 2018; Ma et al., 2019; Yu et al., 2021). In brief, the primary VOCs can be oxidized and/or photolyzed by OH, O$_3$ and NO$_3$ to produce secondary VOCs, e.g., non-/semi-volatile organic compounds: NVOCs/SVOCs, which both further transforms into secondary organic aerosol (SOA) *via* a series of atmospheric processes (Odum et al., 1997; Ng et al., 2007; Heald et al., 2020). It was well known that SOA has strong influences on the radiative forcing and climate change (Sadeghi et al., 2021). On the other hand, active VOCs react with NO$_x$ and radicals *via* an array of photochemical pathways to produce O$_3$. Photochemical Assessment Monitoring Stations (PAMS) have confirmed that totally 57 VOCs, including C$_2$-C$_{10}$ alkanes, alkenes, alkynes and aromatics are extremely contributed to the formation of O$_3$ (US EPA, 1990). Atmospheric O$_3$ shows profound impacts on the atmospheric oxidizing capacity, agriculture production and ecosystem (Liu, 1987; Carter, 1994; Mousavinezhad et al., 2021; Sadeghi et al., 2021). Additionally, O$_3$ and PM$_{2.5}$, together with their VOC precursors can damage human health and lead to many diseases such as cancers, respiratory and nervous systems (Rumchev et al., 2007; Amor-Carro et al., 2020). Therefore, the VOC-related studies can provide scientific-based information for the decision-makers to draw up strategies to control PM$_{2.5}$ and O$_3$.

The long-term VOC emission inventory highlighted that there were significant spatial discrepancies of VOC emissions (Li et al., 2019a). The observation campaign also showed that VOC concentrations varied with the sampling sites. These phenomena were attributed to the fact that VOC concentrations were closely correlated with the land-use types. For instance, the VOC concentrations varied approximately from 20 to 40 ppb at the urban area (Geng et al., 2008; Cai et al., 2010b; Huang et al., 2015; Dai et al., 2017; Liu et al., 2019; Xu et al., 2019; Ren et al., 2020; Wang et al., 2020; Liu et al., 2021), and ~ 90 ppb at the industrial area in Shanghai, China (Zhang et al., 2018; Wang et al., 2021). Kumar et al. (2018) found that the VOC concentration at the urban area was approximately twice higher than that at the rural area in Delhi, India, as the finding of Tang et al. (2008). However, the reported VOC concentrations were widely discussed by single-site measurements, the limited knowledge is available on the multi-site research at a city level. Besides, the land-use types were also related to the VOC sources, especially the anthropogenic sources (Yoo et al., 2015; Chen et al., 2017; Wang et al., 2017; Jookjantra et al., 2022). For example, in Shanghai, China, vehicle-related source was regarded as the predominate VOC source accounting

for 34 % at the urban area (Cai et al., 2010a), while the industrial emission accounted for over 50 % of the measured VOCs near an industrial site (Zhang et al., 2018). In Zhengzhou, China, the solvent utilization was the largest contributor (34 %) at the urban area (Li et al., 2020a), whereas coal and biomass burning was the major source for ambient VOCs (30.6 %) at the Gongshui site surrounded by several manufacturing plants (Li et al., 2019b). Such great discrepancies among the different
70   land-use types results in the fact that it is necessary to perform concurrent multiple-site measurements of VOC characteristics at a city level.

The diversities of VOC concentrations among the different land-use types could affect the ozone and SOA formation potentials (OFP and SOAFP), resulting in the variations of O_3 and SOA concentrations. For instance, Song et al. (2021) found that the OFP values at the commercial and residential areas were approximately twice higher than that at the area
75   dominated by natural vegetation in Xi'an, China, which was in agreement with the finding of Kumar et al. (2018). Such scenario could influence the atmospheric O_3 concentration in that VOCs is an important precursor of O_3 formation. In detail, atmospheric VOCs undergoes degradation to produce oxidants (HO_2 and RO_2), which further oxidizes atmospheric NO, followed by producing NO_2 and the formation of O_3 finally *via* the photochemical pathways (Wang et al., 2017). In terms of SOAFP, there was higher value at the urban area relative to the suburban area, increased by 54.84 % in Beijing, China (Zhan
80   et al., 2021; Liu et al., 2022). This discrepancy further had profound impacts on the concentration, physical property and chemical composition of SOA. As the key precursor of SOA, VOCs can be oxidized to produce the low VOCs, followed by the formation of SOA *via* homogeneous nucleation (Merikanto et al., 2009). Moreover, the partitioning of semi-volatile products from VOCs and oxidants gas-phase photochemical reactions to form SOA (Pankow, 1994; Lim et al., 2010). Additionally, low VOCs are produced *via* the aqueous-phase reactions in atmospheric waters e.g., clouds, fogs, and aerosol
85   water which are largely retained in the particle-phase to generate SOA (Lim et al., 2010).

As the junction of transportation and a center of industry, finance, economy and technology of East China, Shanghai covers an area of 6340 km^2 and the population over 24 million. The expanding urbanization and industrialization jointly aggravate the VOC pollution. Moreover, the O_3 concentration at the urban area in Shanghai increased by ~ 67 % from 2006 to 2015 with the growth rate of 1.1 ppbv pear year (Gao et al., 2017). The maximum 1-hour concentration of O_3 could exceed 380 μg
90   m^{-3} during polluted days (Shi et al., 2015; Gu et al., 2020). Such scenario suggested that O_3 played an important role in atmospheric pollution and Shanghai was suffering from heavy O_3 pollution. Additionally, the large changes of land-use occurred in Shanghai due to the rapid development e.g., many cultivated areas became urban and/or industrial zones, resulting in the diverse land-use types (Tian et al., 2017). Therefore, Shanghai is regarded as an ideal area to perform atmospheric measurements with the different land-use types. However, many studies were mainly focused on the single-site
95   measurements, particularly conducted at the urban site in Shanghai, resulting that the impact of land-use type on VOC characteristics is still unclear to date. Besides, they mainly concentrated on the O_3 characteristics, while the O_3 and SOA formations from VOCs and the relationship between VOCs together with $PM_{2.5}$ and O_3 were rarely analyzed. Given the factors mentioned above, in this study, the concurrent multiple-site and high time-resolution measurement of VOCs with three typical land-use types in Shanghai for their concentrations, sources and ozone and SOA formation potentials were

performed. The objectives of this study are to (1) figure out the VOC characteristics varying with the land-use types, (2) identify the predominate VOC emission sources, and (3) quantitatively evaluate the roles of VOCs in the formation of $PM_{2.5}$ and O_3. The findings could advance our knowledge in the atmospheric characteristics of VOCs and provide more control strategies for policymakers to alleviate atmospheric pollution.

2. Measurements and methods

2.1 Sampling site description

The three sampling sites are located at the different land-use types of Shanghai, China: industrial district (the Jinshan site: JS, 121.18 °N, 30.44 °E), residential and commercial mixed districts (the Pudong site: PD, 121.54 °N, 31.23 °E) and background district (the Qingpu site: QP, 120.98 °N, 31.09 °E) (Fig. S1). The online instruments were 30 m above the ground level to avoid airflow obstruction.

The JS site is located in the Second Jinshan Industrial Area of Shanghai as an industrial site. The site is situated in ~ 20 km southwest of the Shanghai Chemical Industrial Park and Garbage Disposal Incinerator-2. Moreover, a large number of chemical factories, such as rubber factories, paint solvent factories and oil refineries are located within 2 km of the JS site. In particular, Shanghai Petrochemical Industrial Limited Company (one of the largest refining-chemical integrated petrochemical companies in Shanghai) is 1.5 km southeast of the JS site. Additionally, two arterial roads are located 100 and 300 m away from the JS site, respectively. Thus, the land-use type of JS site could be regarded as industrial district (Tab. S1). The PD site is located in the Pudong New Area as an urban site, ~ 59 km northeast of the JS site. The Pudong New Area is the most populous district of Shanghai with a population up to 5.6 million (the Seventh Census of China). The Baosteel Group Corporation, International Cruise Port wharf, Waigaoqiao Shipbuilding LTD and Domestic Waste Incinerator totally are located within 30 km of the PD site. The Yangshan Harbor (the biggest harbor of Shanghai) and Garbage Disposal Incinerator-1 are located in 51 and 37 km southeast of the PD site, respectively. Furthermore, the PD site is surrounded by three main airports of Shanghai, including Hongqiao International Airport, Longhua Airport and Pudong International Airport. In addition, the site is a junction of roads, commercial and financial areas with intense human activities, which is ~ 1.5 km away from Jinxiu Road, Jincai High School, Jinnan High School, and Jincai Experimental Primary School. Therefore, the land-use type of PD site is residential and commercial mixed districts (Tab. S1).

The QP site is located near the southeast of Dianshan Lake where is a tourist attraction in the Qingpu district as a city background site, ~ 50 km northwest of the JS site and 54 km southwest of the PD site. Surrounded by vegetation, the QP site is situated in ~ 7.6 and 4.6 km northeast of the Grand View Garden and Chenguang Garden, respectively. Moreover, this site is 3.6 km northeast of the Qingxi Country Park and 7.5 km southwest of the Zhuxi Garden. Besides, the QP site is close to Hu-Yu Highway. Hence, the land-use type of QP site is considered as background district (Tab. S1). Since the distinct land-use types among the sampling sites were observed, it is quite necessary to perform atmospheric measurements herein.

2.2 Sampling and analysis

The concentrations of VOCs, CO, NO-NO$_2$-NO$_x$, PM$_{2.5}$, and meteorological factors including temperature, wind speed and relative humidity (RH) were measured in one-hour resolution. The sampling campaign was performed simultaneously at the three sites from January 1 to March 31 2019.

At the JS site, the VOCs was collected and analyzed by an online gas chromatography (GC866, Chromato, France) equipped with flame ionization detector (FID). In brief, after the removal of water, the samples were separated for low-carbon (C$_2$-C$_5$) and high-carbon (C$_6$-C$_{12}$) compounds at the temperature of -5℃ and 25℃, respectively. Then the gas was analyzed by FID after high temperature desorption (380℃) and column chromatographic separation. At the PD site, VOCs was measured by gas chromatography (GC580-FID, PE, USA) and TD300 (a transformer driver). The samples were separated at -30℃ after the removal of water. Then the gas was determined by FID, after high temperature desorption (325℃) and column chromatographic separation. At the QP site, VOCs were determined by gas chromatography (GC5000 BTX/VOC, AMA, German) and a flame ionization detector (FID). The samples were condensed for low-carbon (C$_2$-C$_5$) compounds at 15℃ and high-carbon (C$_6$-C$_{12}$) compounds at 30℃. Then the gas was analyzed by FID after high temperature desorption (230℃) and column chromatographic separation. The curve correlation coefficient (R^2) of all of the VOCs were ≥ 0.995. The accuracy of more than 95 % of compounds was ≤ ± 20 %. The precision of all target compounds was ≤ 10 %. Totally 43 species of VOCs were observed, including 16 alkanes, 11 alkenes, 16 aromatics and 1 alkyne. The minimum detection limit (MDL) of most VOC components was ≤ 0.15 ppb (Tab. S2).

The O$_3$, NO-NO$_2$-NO$_x$ were characterized by trace gas instruments (49i ozone analyzer and 42i nitrogen oxide analyzer, produced by Thermo Environmental Instruments Inc., USA) with the detection limits of 0.50 and 0.40 ppb, respectively. PM$_{2.5}$ was monitored by a TEOM 1405-F. The meteorological variables including temperature, RH and wind speed were acquired from each air monitoring station.

2.3 Spatial analysis

The spatial heterogeneity of VOC concentration between two different sites was determined by the coefficient of divergence (COD) (Wongphatarakul et al., 1998; Sawvel et al., 2015). The COD was calculated by Eq. (1):

$$COD_{jk} = \sqrt{\frac{1}{p}\sum_{i=1}^{p}(\frac{x_{ij} - x_{ik}}{x_{ij} + x_{ik}})^2} \tag{1}$$

where x_{ij} presents the mass concentration in i time, j and k are two datasets, p presents the number of observations. The values of COD represented the degree of similarity of the two datasets, i.e., the value of COD approached 1, illustrating that the big difference exist in the two datasets (Song et al., 2017).

2.4 Positive matrix factorization (PMF) model

PMF was a receptor model designed for the source identification of atmospheric pollutants (Li et al., 2015b; Hopke et al., 2016; Pallavi et al., 2019). In brief, it measured the contributions and sources of pollutant by the least squares, and was based on the mass balance instead of the spectrum of source component (Hui et al., 2018). In the PMF 5.0, the mass balance equation was calculated by Eq. (2):

$$x_{ij} = \sum_{k=1}^{p} g_{ik} f_{kj} + e_{ij} \tag{2}$$

where x_{ij} is the jth species concentration in the sample i, g_{ik} represents the species contribution of the kth source to the ith sample, f_{kj} is the jth species fraction from the kth source, e_{ij} is the residual result for jth species in ith sample, p is the number of independent sources (Paatero, 1997). The function Q was an important factor of PMF (Brown et al., 2015), and calculated by iterative minimization algorithm (Hui et al., 2018). The objective function Q was shown in the Eq. (3):

$$Q = \sum_{i=1}^{n} \sum_{j=1}^{m} \left[\frac{x_{ij} - \sum_{k=1}^{p} g_{ik} f_{kj}}{u_{ij}} \right] \tag{3}$$

where u_{ij} is the uncertainty of jth species in the sample i.

The uncertainty of sampling was calculated by the Eq. (4).

$$Unc = \sqrt{(EF \times conc)^2 + (0.5 \times MDL)^2} \quad (conc > MDL) \tag{4}$$

where MDL is the minimum detection limit, EF is the error fraction and can be set to 0.05-0.2 (Song et al., 2007). It was 0.1 in this study. In this study, four to eleven factors were utilized to determine the option solution. Q_{true}/Q_{robust} and and $Q_{true}/Q_{expected}$ are important parameters for characterizing the rationality of the PMF results (Brown et al., 2015). Seven factors were regarded as the optimal solution, comparing the ratios of Q_{true}/Q_{robust}, $Q_{true}/Q_{expected}$ and PMF results. The Q_{true}/Q_{robust} values were set to 1.0 at the three sampling sites. The $Q_{true}/Q_{expected}$ values were 1.3, 1.1, and 1.0 at the JS, PD and QP sites, respectively.

2.5 Potential source contribution function (PSCF) and Cluster

PSCF and Cluster were widely used to determine the back trajectories, source and direction of pollutants (Draxier and Hess, 1998; Hong et al., 2019; Liu et al., 2019), and designed to measure the potential VOC source and primary transport pathway of trace elements (Ashbaugh et al., 1985; Xie et al., 2007; Zheng et al., 2018; Liu et al., 2020).

This study was determined by the 24-h back trajectories (one hour interval) at the height of 500 m via the MeteoInfoMap software. Relevant parameters were acquired from the National Oceanic and Atmospheric Administration. The study area covered by back trajectories was divided into an array of 0.25° × 0.25° grid cell. The higher PSCF indicated that the area was a great contributor to the VOC pollution. The PSCF could be defined as the Eq. (5).

$$PSCF_{ij} = \frac{m_{ij}}{n_{ij}} \tag{5}$$

where the m_{ij} is the number of polluted trajectories through the grid, n_{ij} is all of the trajectories through the grid. In order to distinguish the value of PSCF and increase the accuracy, the weight function W_{ij} was applied to reveal the uncertainty of small values of n_{ij} (Polissar et al., 1999). The W_{ij} could be calculated using the Eq. (6) as follows:

$$W_{ij} = \begin{cases} 1.00 & 80 < n_{ij} \\ 0.70 & 20 < n_{ij} \leq 80 \\ 0.42 & 10 < n_{ij} \leq 20 \\ 0.05 & n_{ij} \leq 10 \end{cases} \tag{6}$$

Therefore, the $PSCF_{ij}$ can be calculated using the Eq. (7) as follows:

$$PSCF_{ij} = \frac{m_{ij}}{n_{ij}} \times W_{ij} = \frac{m_{ij}}{n_{ij}} \times \begin{cases} 1.00 & 80 < n_{ij} \\ 0.70 & 20 < n_{ij} \leq 80 \\ 0.42 & 10 < n_{ij} \leq 20 \\ 0.05 & n_{ij} \leq 10 \end{cases} \tag{7}$$

2.6 Ozone formation potential (OFP)

The photochemical activity of VOCs was normally assessed by the O_3 formation potential (OFP) (Niu et al., 2016). The value of OFP was affected by many factors like meteorological conditions, VOC concentrations and VOC sources. The OFP was calculated by Eq. (8):

$$OFP_i = [conc]_i \times MIR_i \tag{8}$$

where OFP_i is the ozone formation potential of the i species, $[conc]_i$ is the concentration of VOC species i, MIR_i is the maximum incremental reactions of the i VOC species, as reported by Carter (1994).

2.7 Secondary organic aerosol formation potential (SOAFP)

As discussed by Grosjean and Seinfeld (1989), SOAFP could be used to evaluate quantitatively the VOC influences on the secondary aerosol formation based on a variety of assumed interactions between VOCs and OH under the sunlight irradiation (8:00-17:00).

$$SOAFP_i = [VOC_i] \times FAC_i \tag{9}$$

where VOC_i is the concentration of the i VOC species, FAC_i is fraction aerosol coefficient of the i compound. The FAC_i was obtained from the previous studies (Grosjean and Seinfeld, 1989; Zhu et al., 2017; Mozaffar et al., 2020).

2.8 Sensitivity analysis

In order to further understand the relationship between VOCs and PM$_{2.5}$, a gradient model was applied to investigate the sensitivity of PM$_{2.5}$ pollution to the VOC concentration. The Eq. (10) was below:

$$\eta = \frac{\Delta_{\text{VOCs}}}{\Delta_{\text{PM}_{2.5}}}$$ (10)

where Δ_{VOCs} and Δ_{O3} is the concentrations of VOCs and PM$_{2.5}$ in the specific PM$_{2.5}$ gradients, respectively. The characteristic structure and reactivity could influence the contribution of VOCs to PM$_{2.5}$ formation (Cater, 1994). To determine the quantitative relationship between the VOCs and PM$_{2.5}$, the VOCs-sensitivity coefficient (VOCs-S$_{PM2.5}$) was used as the Eq. (11):

$$VOCs\text{--}S_{\text{PM}_{2.5}} = \frac{\Delta_{\text{VOCs}}/B_{\text{VOCs}}}{\Delta_{\text{PM}_{2.5}}/B_{\text{PM}_{2.5}}}$$ (11)

where B_{VOCs} and $B_{PM2.5}$ are the background concentrations of VOCs and PM$_{2.5}$. The PM$_{2.5}$ concentrations below 20 μg m^{-3} were averaged to be the background level (Han et al., 2017). The background concentration of VOCs (B_{VOCs}) was the corresponding VOC concentrations. The higher value of VOCs-S$_{PM2.5}$, the more sensitive VOCs to the PM$_{2.5}$ concentrations. In order to quantify the sensitivity of VOCs to PM$_{2.5}$, VOCs and PM$_{2.5}$ were classified into different groups with a PM$_{2.5}$ concentration interval of 5 μg m^{-3}. It could be calculated by the Eqs. (12-15):

$$y = a \cdot x^{b}$$ (12)

$$\ln y = \ln a + b \cdot \ln x$$ (13)

$$\ln VOCs - S_{PM_{2.5}} = \ln a + b \cdot \ln \frac{\Delta_{PM_{2.5}}}{B_{PM_{2.5}}}$$ (14)

$$\ln \frac{\Delta VOCs}{BVOCs} = k \cdot \ln \frac{\Delta_{PM_{2.5}}}{B_{PM_{2.5}}} + c$$ (15)

where k represents the linear coefficient between $\ln(\Delta_{VOCs}/B_{VOCs})$ and $\ln(\Delta_{PM2.5}/B_{VOCs})$, c is the intercept. This method was appropriate for understanding the sensitivity of VOC concentrations to PM$_{2.5}$.

3. Results

3.1 Characteristics of air pollutants

3.1.1 Data overview

Figure 1 shows the variations of meteorological factors, VOC categories, PM$_{2.5}$ and O$_3$ at the sampling sites. The average temperatures were 8.69 ± 3.24, 9.02 ± 3.24 and 7.73 ± 2.92 ℃, and the mean RHs were 83.77 ± 11.38, 75.37 ± 13.29 and 71.80 ± 9.28 % at the JS, PD and QP sites, respectively. The wind speed at the QP site (4.37 ± 1.47 m s^{-1}) was 2.29 and 1.36 times higher than those at the JS (1.91 ± 0.49 m s^{-1}) and PD (1.30 ± 0.62 m s^{-1}) sites, respectively, indicating the decreased dilution and diffusion conditions at the latter two sites. Besides, the land-use types of the JS (industrial district) and PD (residential and commercial mixed districts) sites could lead to high anthropogenic emission. These phenomena result in the fact that the VOC concentrations at the JS (21.88 ± 12.58 ppb) and PD (21.36 ± 8.58 ppb) sites were higher than that at the QP site (11.93 ± 6.33 ppb). Compared with the relevant measurements performed previously in Shanghai at the same sampling sites, this study generally presented lower VOC concentrations (Cai et al., 2010b; Zhang et al., 2018; Zhang et al., 2020a). In detail, at the JS site, the VOC concentration was approximately 4 times lower than the measurement of Zhang et al., (2018) (94.14 ppb). At the PD and QP sites, the results in this study were slightly lower than those reported by Cai et al. (2010b) (24.3 ppb) and Zhang et al. (2020a) (15.41 ppb). A variety of control strategies, such as prohibiting of fireworks in the open air, improving VOC detection standards and strengthening control technology were implemented, thus resulting in the low VOC concentrations herein. Particularly, the policy of "one factory, one strategy", targeted at mitigating VOC emissions, was published by Shanghai government in 2018.

The two prominent peaks of VOC concentrations were observed at the JS site on 23 January and 11 March, respectively. The highest VOC concentration appeared on 11 March with a value of 84.49 ppb. This phenomenon might be attributed to the leaking of chemical factories. The second highest VOC concentration was observed on 23 January with a value of 77.71 ppb which was 38.85 and 57.07 % higher than those at the PD and QP sites, respectively. According to the Shanghai Municipal Bureau of Statistics (http://tjj.sh.gov.cn), the traffic flow in January was ~ 10 % higher than that in the following two months. Such scenario was likely due to the Spring Festival Travel rush, i.e., population travel intensively occurred around the Chinese Spring Festival. Moreover, there were pronounced in the industrial production in January compared with those in February (~ 36 % uplift) and March (~ 6 % uplift) (http://tjj.sh.gov.cn). The phenomena could be responsible for the elevated VOC emissions. Additionally, the lowest WS was observed on 23 January with the value of 0.85 m s^{-1}, which was adverse to dispersive dilution and convection of VOCs, causing high concentrations of VOC at the JS site (Kumar et al., 2018).

During the observation period, the average PM$_{2.5}$ values were 45.57 ± 27.59, 48.51 ± 27.22 and 40.27 ± 27.78 μg m^{-3}, and the mean O$_3$ concentrations were averaged to be 73.59 ± 23.59, 57.48 ± 20.49 and 99.30 ± 24.00 μg m^{-3} at the JS, PD and QP sites, respectively. VOCs was found to be positively correlated with PM$_{2.5}$, and the spearman correlation coefficients ($R_{Spearman}$) were 0.72, 0.74 and 0.34 at the JS, PD and QP sites, respectively. It was well documented that the elevated VOC concentrations led to the increasing rate of PM$_{2.5}$ production *via* photochemical oxidation, gas-particle partition and/or heterogeneous absorption (Seinfeld et al., 2001; Yang et al., 2015; Han et al., 2017). Moreover, PM$_{2.5}$ and VOCs present similar emission sources. For example, traffic exhaust was proven as the predominant contributor for both of them (Li et al., 2009; Cai et al., 2010a; Cai et al., 2010b; Wang et al., 2013; Kuo et al., 2014; Liu et al., 2019). However, the VOC concentrations were negatively correlated with O$_3$ ($R_{Spearman}$ = -0.39 at the JS site, $R_{Spearman}$ = -0.50 at the PD site and $R_{Spearman}$

265 = -0.40 at the QP site, respectively). Lots of factors including NO_x levels, sunshine duration, temperature and relative humidity not only the emission of precursors, impacted on the surface O_3. Li et al. (2019b) emphasized that the absolute concentration of precursor was not the only factor during the O_3 formation in Zhengzhou, China.

3.1.2 Chemical compositions

The VOC compositions at the JS, PD and QP sites are presented in Fig. 2. During the observation campaign, 43 VOC species
270 including 16 alkanes, 11 alkenes, 16 aromatics and 1 alkyne were measured and the contributions of total VOCs (TVOCs) > 1 % were marked. The most abundant specie was alkanes, followed by aromatics at the JS, PD and QP sites. The contributions of alkenes and alkyne were comparable at the above sites. Specially, ethane, propane, iso-butane, n-butane, ethylene, benzene, toluene and ethyne were the abundant individual species and they totally contributed to greater than 75 % of the TVOCs.

275 Among four major organic classes, the fractions of alkanes were 49.32, 71.48 and 60.88 % at the JS, PD and QP sites, respectively, in line with the previous result (59.36 %) (Zhang et al., 2020a). Such high fraction of alkanes can be attributed to their widespread emission sources and long atmospheric lifetimes. In terms of VOC species, the ethane, propane and C_4-C_6 branches alkanes contributed greatly to the alkanes at the sampling sites, in accordance with the findings of Zhang et al. (2020a) and Song et al. (2021).

280 The second-largest group was aromatics accounting for 21.00, 10.70 and 13.75 % at the JS, PD and QP sites, respectively. As reported by Cai et al. (2010b), the aromatics at the Xujiahui site in Shanghai, China accounted for 24.9 % of the TVOCs which was slightly higher than the results obtained in this study. It is interesting to note that the dominating compounds of aromatics were toluene, m/p-xylene, benzene, ethylbenzene and o-xylene (BTEX), in line with the results at some Chinese cities such as Shanghai (Zhang et al., 2018) and Xi'an (Song et al., 2021).

285 The alkenes accounted for 15.30, 10.13 and 10.57 % at the JS, PD and QP sites, respectively, and the discrepancies of alkenes contributions to TVOCs among three sites were narrow. The ethene, propylene and butene were predominant compounds in the composition of alkenes, and their contributions were comparable to the results of Shao et al. (2016). The alkyne contributed 14.38, 7.69 and 14.80 % on the TVOCs at the above sites. Relative to the result reported by Liu et al. (2017) in Hangzhou, China, the contribution of alkyne was comparable to the present study, accounting for 16.6 % of the
290 TVOCs.

3.1.3 "Weekend effects"

The "weekend effects" of VOCs at the JS, PD and QP sites are shown in Fig. 3. On the weekdays, the average VOC concentrations were 21.03 ± 2.66, 22.00 ± 4.88 and 11.09 ± 1.58 ppb at the JS, PD and QP sites, respectively. The morning peak values were observed during the rush-hour traffic at 8:00 to 10:00 LT, reaching 26.61, 35.11 and 13.54 ppb,
295 respectively due to the morning traffic. The peak was more significant at the PD site than those at the JS and QP sites, illustrating that the significant impact of land-use type, leading to the high vehicle emission at the PD site. During the

rush-hour traffic at 18:00 to 21:00 LT, the VOC concentrations also tended to increase, and the evening peak values were 18.46, 20.82 and 10.22 ppb at the JS, PD and QP sites, respectively. Such scenario could be attributed to the strong influence of the vehicle exhaust. The VOC concentrations dropped to the minimum at the 16:00 LT with the values of 16.96, 15.62 and 8.77 ppb at the JS, PD and QP sites, respectively. The strong radiation, high temperature and boundary layer resulted in the most intense air convection condition and promoted the photochemical loss and dilution of VOCs, leading to the decreased VOC concentration (Zhang et al., 2018). On the weekends, the JS site exhibited the highest average VOC concentration of 20.36 ± 2.23 ppb, followed by the PD and QP sites with the concentrations of 19.96 ± 2.37 and 10.96 ± 0.67 ppb, respectively. The VOC concentrations on the weekends were 3.31, 10.19 and 1.19 % lower than those on the weekdays at the JS, PD and QP sites, respectively. Similarly, the elevated VOC concentrations on the weekdays were found in the other studies including Shanghai, China (Geng et al., 2008), Sacramento, California (Murphy et al., 2007) and Los Angeles, California (Nussbaumer and Cohen, 2020), due to the low anthropogenic activities occurring on the weekends, reflecting the low VOC emission (Murphy et al., 2007). The minimum VOC concentrations on the weekends appeared on the 16:00 LT at the JS and PD sites and 15:00 LT at the QP site, respectively, with the values of 17.14, 17.56 and 10.33 ppb which occurred around the similar time as those on the weekdays.

3.1.4 Discrepancy of clean and haze day

Referring to the previous documents (Li et al., 2017; Hui et al., 2019), haze pollution was defined as the condition with visibility < 10 km and RH < 80 %. During the observation period, there were three sequential haze pollution events at the three sites on the basis of this criteria, i.e., 18 to 25 January, 23 February to 3 March and 21 to 26 March. The VOC concentrations between the clean and haze days are shown in Fig. 4. The VOC concentrations on the clean days were averaged to be 20.53 ± 12.10, 19.29 ± 7.60 and 11.04 ± 6.67 ppb at the JS, PD and QP sites, respectively. For the haze days, the VOC concentrations increased by 27.15, 32.85 and 22.42 % at the above sites. Wu et al. (2016) also emphasized the increased VOC concentrations during the haze days relative to clean days in Beijing, China. Obviously, the 'haze-clean' differences of VOC concentrations were more significant at the JS and PD sites compared with the QP site. Such scenario could be attributed to the locations of JS and PD sites which led to high anthropogenic emissions and low wind speed and implicated stagnant weather conditions, therefore inducing the severe haze pollution. In detail, the 'clean-haze' discrepancy was dominated by the aromatics (m-ethyltoluene, p-ethyltoluene, ethylbenzene, 1, 2, 4-trimethylbenzene) at the JS and PD sites, as reflected by the 44.54 and 36.05 % higher concentrations on haze days relative to clean days. The above VOC compounds were related with the industrial production, painting/coating and vehicle exhaust, and elevated concentrations reflected the concentrated emission sources. Zhang et al. (2021) studied the VOC characteristics during the haze pollution in Zhengzhou, China, and showed that aromatics present an upward tendency (~ 34.04 % uplift) on the haze days, which was slightly lower than the results shown herein. At the QP site, alkanes (2, 2, 4-trimethylpentane, n-hexane, n-heptane) presented significant 'clean-haze' discrepancy (~ 36.58 % uplift), implying the great impacts of vehicle exhaust and fuel evaporation. Hui et al. (2018) also observed the elevated concentration of alkanes during the haze days in Wuhan, China, and

found that there were 37.28 % increment of alkanes, which was comparable to the result in the present study. Thus, it could be deduced that, the haze occurrence is mainly associated with vehicle exhaust, industrial production and painting/coating at the JS and PD sites, whereas the vehicle exhaust and fuel evaporation at the QP site. Such deduction on the source of haze events agreed well with the studies about the haze pollution in Shanghai, China (Li et al., 2019b; Wei et al., 2019).

3.2 Source apportionment

3.2.1 Special VOC ratio analysis

Different VOC species have different sources, and the ratio of different species can be used to preliminary distinguish the emission sources (An et al., 2014). Herein, the characteristics of toluene/benzene (T/B), *iso*-pentane/*n*-pentane (P/P) and *m, p*-xylene/ethylbenzene (X/E) varying at the sampling sites are utilized to identify the VOC sources. The results are shown in Fig. 5 and Fig. S2-4.

It is well documented that the varied VOC sources could be identified by the different T/B ratios (Song et al., 2021). The mean T/B ratios were 4.59 ± 4.3 and 1.61 ± 0.79, with the pearson correlation coefficients ($R_{Pearson}$) of 0.41 and 0.65, respectively at the JS and PD sites. The most of the ratios (68.89 and 84.15 %) distributed the range of 0.9-2.2 and 1.4-5.8, suggesting that vehicle emissions and industrial emissions exerted the significant impact on VOC concentrations (Fig. 5a-b), which was well agreement with the previous studies (Dai et al., 2013; Zhang et al., 2013; Mo et al., 2015; Shi et al., 2015; Yao et al., 2015; Deng et al., 2018). The average ratio at the QP site was 1.01 ± 0.66 ($R_{Pearson} = 0.70$) with 43.02 % of T/B ratios distributing the range of 0.9-2.2 and 0.2-0.4, suggesting that vehicle emissions and burning emissions contributed significantly to VOC pollution (Fig. 5c) (Li et al., 2011; Dai et al., 2013; Zhang et al., 2013; Yao et al., 2015; Mo et al., 2016; Deng et al., 2018). The temporal variations of T/B ratio and TVOC concentrations are shown in Fig. S2. The T/B ratios were mainly located in the scopes of vehicle emission and industrial source at the JS and PD sites when the VOC concentrations were high, respectively, while the specific values at the QP site were only concentrated in the scope of vehicle emission. Such scenario showed that vehicle exhaust was a significant contributor to the VOC pollution at the sites we studied, and VOC concentrations were less influenced by the industrial emission at the QP site relative to the JS and PD sites, due to the land-use type of QP site where is normally taken as a city background site and far from the industrial area.

The fossil fuel-derived sources (vehicle exhaust, fuel evaporation and coal combustion) could be further distinguished by the P/P ratio. *Iso*-pentane and *n*-pentane have similar atmospheric lifetimes, therefore varied with a similar trend and were highly correlated ($R_{Pearson} = 0.91$, 0.91 and 0.81 at the JS, PD and QP sites, respectively), indicating the similar emission sources of two compounds (Jobson et al., 1998; Yan et al., 2017). Lower P/P ratios (0.56-0.80) are often identified for coal combustion (Li et al., 2019c), and the P/P ratios in the range of 2.2-3.8 are characterized by vehicle emission (Liu et al., 2008; Wang et al., 2013). The average P/P ratios between the iso-pentane and *n*-pentane were 0.96 ± 0.30, 1.36 ± 0.22 and 2.46 ± 1.49 at the JS, PD and QP sites, respectively (Fig. 5d). The result at the QP site was comparable with that measured at a Pearl River tunnel (2.93), suggesting that the vehicle emission was an important VOC source (Liu et al., 2008). The lower ratios at the JS

and PD sites indicated that VOC concentrations were affected by coal combustion sources. The temporal variations of P/P ratio and TVOC concentrations are shown in Fig. S3. The P/P ratios were distributed within the range of 2.2-3.8 at the sampling sites when the VOC concentrations were high, indicating the great impact of vehicle emission on VOC pollution, which was in agreement with the report of Song et al. (2021).

Besides the local emissions influencing the VOC pollution characteristics, regional transport has been probed as a potential VOC source. Herein, the ratio of X/E was used to evaluate the transport impacts. *M, p*-xylene and ethylbenzene are found to be similar in emission sources, while the former exhibits ~ 3 times greater reactivity toward OH radical than the latter (Nelson and Quigley, 1983; Chang et al., 2006; Vardoulakis et al., 2011). Hence, lower X/E ratios normally suggested more significant air mass aging, that is, more influences from external transport. The X/E ratios were averaged to be 2.33 ± 0.37 ($R_{Pearson}$ = 0.98), 2.18 ± 0.42 ($R_{Pearson}$ = 0.97) and 2.03 ± 1.52 ($R_{Pearson}$ = 0.74) at the JS, PD and QP sites, respectively (Fig. 5e). The results showed that the X/E ratios were slightly lower at the QP site relative to the JS and PD sites, indicating that there were less primary emissions from anthropogenic sources at the QP site The temporal variations of the X/E ratio and TVOC concentrations are shown in Fig. S4. When the VOC concentrations were high, the X/E ratios were approximately 2.3, 2.5 and 1.8 at the JS, PD and QP sites, respectively. Obviously, the X/E ratio was lower at the QP site than those at the JS and PD sites. In particular, the high VOC concentration (27.17 ppb) was observed in 7 February at the QP site, corresponding to the minimum X/E ratio (0.27), while the X/E ratios were 3.07 and 1.95 at the JS and PD sites, corresponding to the VOC concentrations of 12.45 and 22.45 ppb. Such results illustrated that the impact of external transport during the VOC pollution was greater at the QP site compared with the JS and PD sites.

3.2.2 The PMF analysis

The PMF analysis can quantitatively determine the VOC source contributions (Hui et al., 2019). In this study, 39 VOC species were put into the PMF model, followed by the output of seven resolved factors including vehicle exhaust, industrial source, LPG usage, paint solvent, fuel production and evaporation, coal combustion and biomass burning. The source profiles of the resolved factors by the PMF model are shown in Fig. 6.

Vehicle exhaust was characterized by the high proportions of alkanes, some alkenes and certain percentage of aromatics (benzene, xylene and trimethylbenzene) (Liu et al., 2008; Cai et al., 2010a; Ling et al., 2011; An et al., 2017; Hui et al., 2018). In this study, the high contributions of the ethane (69.59 and 48.01 %), *iso*-butane (35.14 and 26.12 %) and some alkenes especially the propylene (34.72 and 19.74 %) and *trans*-2-butene (50.49 and 17.40 %) at the JS and PD sites and the ethane (42.41 %), ethylene (49.14 %) and ethyne (45.94 %) at the QP site were observed. These compounds are widely regarded as vehicular emission tracers (Cai et al., 2010a; Ling et al., 2011; An et al., 2017; Hui et al., 2018). The contributions of vehicle exhaust were calculated to be 23.18, 33.37 and 32.12 % at the JS, PD and QP sites, respectively. The relevant high results indicate that vehicle exhaust was the predominant source of VOCs, in accordance with the results of T/B and P/P ratios mentioned above. Shanghai owns the motor vehicles more than 4.4 million in 2019. Vehicle exhausts had been proved to be one of the main causes of the local air pollution in Shanghai (Huang et al., 2015; Dai et al., 2017; Liu et al.,

395 2019; Cai et al., 2010b).

Industrial emission was featured by the high percentage of aromatics (benzene, toluene and trimethylbenzene) and certain percentages of alkanes and alkenes (Guo et al., 2011; Dumanoglu et al., 2014; Sun et al., 2016). At the JS and PD sites, the high contributions of *n*-nonane (17.84 and 33.99 %), benzene (13.89 and 39.16 %), toluene (21.11 and 19.54 %), trimethylbenzene (94.18 and 84.05 %), hexane (14.81 and 38.96 %) and ethylene (14.99 and 36.91 %) were observed. It was

400 widely acknowledged that asphalt application could release *n*-nonane (Brown et al., 2007; Liu et al., 2008). Moreover, benzene and toluene are primarily applied for industrial solvent production, and trimethylbenzene is frequently used in manufacturing (Morrow, 1990; Ling et al., 2011). Therefore, the recognized factor can be identified as industrial source. Industrial events were calculated to contribute 22.39 % and 18.81 % to VOCs at the JS and PD sites, respectively, indicating the considerable contributions of industrialization next to the aforementioned traffic factors. The QP site was far away from

405 the industrial regions, and therefore was less influenced by industrial factors compared with JS and PD sites.

Coal combustion factor was characterized by C_2-C_3 alkenes such as ethylene and propylene, some alkanes, ethyne, benzene and ethylbenzene (Liu et al., 2008; Ling et al., 2011; Song et al., 2018). Moreover, the proportions of propene, *n*-hexane, *n*-heptane and toluene were low, but these compounds could not be neglected yet (Hui et al., 2018). The PMF analysis illustrated that coal combustion was the third-largest source of VOCs at the three sites. Coal combustion was responsible for

410 14.95 % and 13.85 % of the VOC emission at the PD and QP sites, respectively. However, the contribution reached up to 21.48 % at the JS site, reflecting more frequent fossil usage in the industrial area of Shanghai.

LPG usage was determined by some alkanes (propane, *n*-butane and iso-butane) and alkenes (ethylene, propylene and butene). There were high proportions of propane (21.24 and 14.41 %), *n*-butane (15.53 and 13.79 %), *iso*-butane (12.61 and 11.40 %), ethylene (31.18 and 10.08 %) and propylene (34.94 and 31.38 %) observed at the JS and PD sites, coupled with

415 *iso*-butane (43.88 %), propylene (25.08 %) and *cis/trans*-2-butene (53.10 and 57.65 %) at the QP site, highlighting the LPG-related sources (Yang et al., 2013; Lyu et al., 2016). Herein, LPG usage accounted for 13.17, 14.76 and 12.14 % of the VOCs monitored at the JS, PD and QP sites, respectively. At the end of 2015, the amount of LPG users about household and catering achieved 3.3-6.5 million in Shanghai (Hui et al., 2018; Zhang et al., 2018a). Overall, LPG usage was one of the important VOC sources at the sampling sites.

420 Fuel production and evaporation could be identified by C_3-C_7 alkanes, especially n-pentane and iso-pentane (Zheng et al., 2020), the C_3-C_5 alkenes such as *trans/cis*-2-butene (Geng et al., 2009; Hui et al., 2018; Zhang et al., 2018a; Zheng et al., 2020) and some aromatics (Liu et al., 2008; Xiong and Du, 2020). There were high contributions of *n*-pentane (37.94, 25.20 and 71.95 %), *iso*-pentane (41.45, 28.18 and 23.16 %) and butene (26.73, 70.83 and 22.52 %) at the JS, PD and QP sites, respectively. The contributions of some aromatics such as benzene at the JS site (44.08 %), isopropylbenzene at the PD site

425 (66.71 %) and 1, 2, 4-trimethylbenzene at the QP site (32.90 %) were also high. It was well documented that alkanes like n-pentane and iso-pentane were gasoline tracers, and some alkanes and aromatics could evaporate from the unburned fuels (Guo et al., 2004; Liu et al., 2008; Wang et al., 2013; Xiong and Du, 2020). The VOC contributions from fuel production and evaporation were calculated to be 4.62, 10.35 and 20.15 % at the JS, PD and QP sites, respectively.

Paint solvent usage was normally characterized by C_6-C_8 alkanes and some aromatics like toluene, ethylbenzene and *x/p*-xylene (Wang et al., 2013; An et al., 2017; Hui et al., 2018; Song et al., 2019a). There were high contributions of toluene at the JS site (65.90 %), toluene and ethylbenzene at the PD site (47.95 and 33.85 %) and *x/p*-xylene at the QP site (24.69 %), respectively. Herein, emission factors that meet these characteristics were identified as paint solvent usages, which accounted for 15.15, 7.77 and 10.36 %, respectively at the JS, PD and QP sites.

Biomass burning was distinguished by the isoprene and some aromatics (Schauer et al., 2001; Liu et al., 2020; Yang et al., 2023). Factors that coincide with the specific characteristic were regarded as biomass burning in this study. Our analysis showed that the contribution of biomass burning to VOC concentrations was 11.39 % at the QP site. However, this emission factor could not be reproduced at the JS and PD sites, implying the limited impacts of biomass burning in the population- and industrialization-concentrated areas that were primarily controlled by the anthropogenic emissions.

3.2.3 Back trajectories and PSCF results

Besides the direct impact of local source, regional transport could also contribute to VOC pollution (Hui et al., 2018). The 24-h backward trajectories, the PSCF results and the VOC proportion of each trajectory throughout the observation at the JS, PD and QP sites are shown in Fig. 7. There were 6 clusters (northern trajectories: Cluster 1 + 2; eastern trajectories: Cluster 3; southern trajectories: Cluster 4; southwestern trajectories: Cluster 5; northwestern trajectories: Cluster 6) at the JS site, as shown in Fig. 7a. The contributions of northern trajectories to the total trajectories (Fig. 7a left) and that of the northern pollution trajectories to the total pollution trajectories (Fig. 7a right) were significantly higher than those of the other four cluster trajectories, comprising 45.74 and 46.46 %, respectively (Tab. 1). Identified as the north direction cluster, the north long-distance trajectory (Cluster 1) and short-distance trajectory (Cluster 2) accounted for 16.67 and 29.07 % of the VOC transportation. The results indicated that the VOC concentrations at the JS site was mainly impacted by the trajectories from the junction of the Bohai Sea, Shandong Province, the East China Sea and Jiangsu Province in addition to the local emission. The contributions of VOCs by each air mass trajectories indicated that alkanes tended to dominate the transported VOC community at the JS site due to its weak reactivity in the long-range transport.

The air mass trajectories could be cluster into northern trajectories (Cluster 1 + 2), northeastern trajectories (Cluster 3), southeastern trajectories (Cluster 4), southwestern trajectories (Cluster 5) and northwestern trajectories (Cluster 6) at the PD site, as shown in Fig. 7b. It is evident that the contributions of northern (Cluster 1) and northeastern (Cluster 3) trajectories to the total trajectories (Fig. 7b left) and that of the northern and northeastern pollution trajectories to the total pollution trajectories (Fig. 7b right) were greatly higher than other four cluster trajectories, accounting for 52.23 and 54.72 % of VOC concentrations, respectively. The results suggested that VOCs at the PD site was significantly influenced by the pollution transportation from East China Sea, Zhejiang Province and Jiangsu Province, coupled with the local sources. The proportions of VOCs by each air mass trajectories indicated that alkanes and alkenes both contributed to the transported VOC community at the PD site.

At the QP site (Fig. 7c), the trajectories were clustered into the northern trajectories (Cluster 1 + 2), northeastern trajectories

(Cluster 3), southeastern trajectories (Cluster 4), southwestern trajectories (Cluster 5) and northwestern trajectories (Cluster 6). The proportion of northeastern trajectories to the total trajectories (Fig. 7c left) and that of northeastern pollution trajectories to the total pollution trajectories (Fig. 7c right) were higher than those of the other trajectories, accounting for 31.87 and 27.81 % of the VOC concentrations, respectively. This result indicated that the concentration of VOCs was mainly impacted by the northeastern trajectory from the junction of East China Sea, Zhejiang Province and Jiangsu Province in addition to local sources. Although the contribution of Cluster 2 was relatively small, the VOC concentration was the highest, reaching 23.63 ± 10.75 ppb (Tab. 1). Therefore, attention should be paid to the long-distance transmission of highly polluting from Beijing, Tianjin and Liaoning Province. The alkanes contributed most of VOCs in air mass trajectories at the QP site, which was in line with the results of the JS site.

The region with high PSCF levels indicates highly potential regional transport sources (Hui et al., 2018). Based on the PSCF results, at the JS and QP sites, high values were observed in the north of Shanghai. At the PD site, high values were observed in the northeast of Shanghai. All three sampling sites presented that the highest PSCF levels appeared in areas near the JS, PD and QP sites, suggesting that local source was a significant contributor to the VOC pollution compared with regional transport.

3.3 Ozone and SOA formation potentials

3.3.1 Ozone formation potential

The atmospheric VOCs was considered as the important precursor of O_3 due to their photochemical reactivity (Alghamdi et al., 2014; Kumar et al., 2018). Fig. 8 displays the OFP contribution proportions of the primary VOC categories and species varying with sampling sites. Hereby, the OFPs were calculated to be 50.89 ± 2.63, 33.94 ± 1.52 and 24.26 ± 1.43 ppb for the VOCs measured at the JS, PD and QP sites, respectively. The photo-induced transformation of VOCs could account for 69.15, 59.05 and 24.43 % of the O_3 concentrations in the above sampling sites (OFP values/O_3 concentrations). The VOC-related O_3 contributions were lower than those in Delhi, India (Kumar et al., 2018), and Chinese cities like Shanghai (Zhang et al., 2018a), Wuhan (Hui et al., 2018), Taiwan (Vo et al., 2018), Nanjing (Mozaffar et al., 2020) and Xi'an (Song et al., 2021). The relatively low OFP values were related with the low VOC concentrations in this study (Tab. S3). The predominate OFP contributor was alkenes especially ethylene and propylene, which exhibited the considerable photochemical reactivity, accounted for 50.21, 49.39 and 60.00 % of the OFPs at the JS, PD and QP sites, respectively (Li et al., 2019b). Such levels were generally comparable with the result obtained in Shanghai, China by Zhang and co-workers (2018), comprising 57 %. Moreover, the high photochemical reactivity of aromatics (Li et al., 2019b), especially the toluene, *o*-xylene and *m/p*-xylene, makes them become the second largest contributor of OFP, in accordance with the finding of Hui et al. (2018). The fraction of aromatics therein accounted for 33.59, 23.21 and 20.02 % of the OFPs at the JS, PD and QP sites, respectively. In comparison, the contributions of alkanes and alkyne were much lower, accounting for 13.11 and 3.09 % at the JS site, 22.90 and 4.50 % at the PD site and 13.07 and 6.91 % at the QP site, respectively. These results indicated that

the VOC photochemical reactivity was closely related to the contribution of O_3 formation which was in agreement with other studies (An et al., 2014; Guo et al., 2017; Hui et al., 2018). Hence, alkenes and aromatics played crucial roles in the formation of O_3. According to the source identification results discussed above, the relevant emission sources, which are thought to be the industrial production and vehicle exhaust at the sampling sites, should be controlled in priority.

3.3.2 SOA formation potential

The close linkages between VOCs and new particle formation induced the quantitative discussion on SOAFP (Chen et al., 2007; Guo et al., 2017; Tan et al., 2018), and the Grosjean's methodology has been widely recommended as the standard reference (Fig. 9). Following the reported methods, the SOAFP was calculated only for daytime (8:00-17:00 LT) to avoid the emission from the human activities during nighttime (Grosjean and Seinfeld, 1989; Zhang et al., 2020b). During the observation campaign, the SOAFP was averaged to be 1.00 ± 2.03, 0.46 ± 0.88 and 0.41 ± 0.58 μg m^{-3} for the VOCs measured at the JS, PD and QP sites, respectively. Such levels were comparable with those obtained in Jinan, China (Zhang et al., 2017) and Taiwan (Vo et al., 2018), China, while higher than that of Nanjing, China (Mozaffar et al., 2020) (Tab. S3). The SOAFP values accounted for 2.19, 0.95 and 1.02 % of the PM$_{2.5}$ concentrations at the above sampling sites (SOAFP values/PM$_{2.5}$ concentrations), all of which were lower than the results in Nanjing, China (3.46 %) (Mozaffar et al., 2020) and Wangdu, China (8.4 and 17.84 % under high-NO$_x$ and low-NO$_x$ conditions, respectively) (Zhang et al., 2020b). The aromatics was determined to be the main SOA contributor, accounting for 86.07, 96.21 and 86.38 % at the JS, PD and QP sites, respectively, in accordance with the findings in Jinan, China (Zhang et al., 2017). The top five abundant VOC species were toluene, x/p-xylene, ethylbenzene, benzene and o-xylene at the above sites. Toluene was determined to be the most abundant VOC specie for SOA formation, with the SOAFP values of 9.31, 3.38 and 2.06 μg m^{-3} at the JS, PD and QP sites, respectively, in agreement with the results of Mozaffar et al. (2020). Obviously, the value at the JS site was significantly higher than those at the PD and QP sites, due to a large number of chemical factories surrounding the JS site, resulting in the high concentration of VOCs especially the aromatics (Hui et al., 2018). Therefore, to achieve the better SOA reduction effects, the concentration of aromatics should be controlled in priority in Shanghai, and more efficient strategies should be developed to limit the emissions of industrial emissions.

4. Discussion

In this section, the effects of land-use type on VOC concentrations, sources and ozone and SOA formation potentials are discussed. Previous studies pointed out that the VOC characteristics (e.g., concentrations and diurnal/weekly variations) and sources varied with the land-use types (Yoo et al., 2015; Jookjantra et al., 2022). Further, the discrepancies of VOC characteristics among the land-use type could affect the ozone and SOA formations (Cai et al., 2010a; Cai et al., 2010b; Jookjantra et al., 2022). Herein, the JS site is located in the Second Jinshan Industrial Area of Shanghai as the industrial district, and surrounded by many chemical factories. The PD site is located in the Pudong New Area as the residential and

525 commercial mixed districts, and surrounded by residences and administrative areas. The QP site is located near the southeast of Dianshan Lake as the background district, and surrounded by many farmlands and forests (Tab. S1). Since the distinct land-use types among the sampling sites were observed, it is highly desirable to discuss the effects of the land-use type on concentrations, sources and O_3 and SOA formation potentials of VOCs in Shanghai.

4.1 The effect of land-use type on VOC concentrations

530 The mean VOC concentrations at the JS (21.88 ± 12.58 ppb) and PD (21.36 ± 8.58 ppb) sites were 1.83 and 1.79 times higher than that at the QP site (11.93 ± 6.33 ppb), implicating the impact of land-use type. In more detail, the JS and PD sites are located at the industrial and urban regions with numerous anthropogenic activities. The enhanced emission strengths at the JS and PD sites could induce severe atmospheric pollution e.g., haze and O_3 pollution (Cai et al., 2010a, b; Zhang et al., 2018). Further, the meteorological conditions including ambient temperature and sunlight irradiance changed, the dispersive

535 dilution and convection phenomenon decreased, which contributed to high VOC concentrations (Kumar et al., 2018). By contrast, the emission strength dropped at the QP site as a consequence of the land-use type of this site (background district). Besides, the land-use types could not only affect the VOC concentrations but also compositions. Specifically, the JS site exhibited higher fractions of aromatics and alkenes, particularly toluene and propylene, than those at the PD and QP sites. This result did necessarily correlate with the fact that the JS site is close to the industrial area with heavy industrial emissions

540 (the dominating source of toluene and propylene), as reflected by the increased toluene and propylene proportions (Zhang et al., 2018; Hui et al., 2019; Li et al., 2019b). However, the contribution of ethane at the JS site was ~ 50 % lower than those at the PD and QP sites. As is well known that ethane is typically tracer of incomplete combustion especially vehicle emission (Guo et al., 2011). It was thus supposed that the vehicle emission exerted a relatively weak influence on VOC emission at the JS site (23.18 %), as compared to the PD (33.37 %) and QP sites (32.12 %). The fraction of alkanes especially the propane

545 was remarkable in the land-use type with residential and commercial activities (the PD site). This site is the junction of roads, metros, commercial and financial areas that had a significant impact on the enrichment in vehicle source and hence could have participate in the high contribution of alkanes (Cai et al., 2010a; Ling et al., 2011; An et al., 2017; Hui et al., 2018). The fraction of alkyne at the PD site was 1.88 and 1.75 times lower than those at the JS and QP sites, which might be caused by the weak combustion sources including chemical- and bio-fuels burning (Zhu et al., 2016; Li et al., 2019b). Note that the

550 distinct spatial heterogeneity of VOCs was also observed with the highest value of the coefficient of divergence (COD = 0.36) between the JS and QP sites, followed by the PD and QP sites (COD = 0.33), with that between the JS and PD sites (COD = 0.20) being the lowest. A greater COD value means less redundancy of the data between two sites (Ma et al., 2019). Hence, the spatial heterogeneity of VOCs between the JS and PD sites was narrow, while the QP site was largely different from other two sites. This result was ascribed to the fact that there were similar pollutant concentrations, meteorological factors,

555 emission intensities and atmospheric conditions at the JS and PD sites, while these indexes in the QP site were rather different from those of the other sites.

The VOC diurnal variations were analyzed with respect to each of the land-use types. The result showed that the VOC concentration in the early morning (5:00 LT) at the JS site was 17.06 and 52.91 % higher than those at the other two sites, which was attributed mostly to the land-use types. There were a large number of rubber factories, paint solvent factories and oil factories surrounding the JS site, whereby some factories usually worked continuously for 24 hours, thus inducing the increased VOC concentrations. Compared with the other studies (Velasco et al., 2007; Zhang et al., 2018; Wang et al., 2021), no evident bimodal features can be observed at the sampling sites. The industrial processes and biogenic-related emission surrounding the sampling sites also had great impact on the VOC variations except for the traffic exhaust, which was the potential reason for such scenario (Yoo et al., 2015). In addition to the diurnal variations, the "weekend effects" of VOCs also appeared to be variable among the different land-use types. Specifically, at the JS site, there were narrow discrepancies of VOC concentrations between the weekdays and weekends except for the rush hour in the morning, which was related to the influence of the full-day operation of industrial processes. At the PD site, the highest value during the morning peak on the weekends (26.03 ppb) was lower than that on the weekdays (35.11 ppb), decreased by ~ 25.86 %, suggesting that there were obvious anthropogenic sources especially the vehicle exhaust. At the QP site, the elevated VOC concentrations (~ 18.69 % uplift) were presented during the 18:00-20:00 LT on the weekends relative to the weekdays. The phenomenon might be associated with the joint effect of VOC intensive emissions by anthropogenic activities at the QP site on the weekends in that this site is located around the Dianshan Lake where is a tourist attraction.

4.2 The effect of land-use type on VOC sources

VOC sources in this study were sensitive to the local emission with the different land-use types. Specifically, the vehicle exhaust was responsible for nearly one third of the VOC emission and was a primary source of VOCs. It is interesting to note that the vehicle contribution was expected to be lower at the JS site than those at the PD and QP sites due to the density of automobiles per unit area. This finding reflected the fact that the JS site is located in the industrial regions favouring the contribution accumulations of industrial production and coal combustion (Yoo et al., 2015). As reported, vehicle emission was a dominating VOC source in other cities, and the contributions were higher than 20 % except in Calgary, Canada (17.2 %) (Fig. 10). Therefore, the effective and continuous control strategies on vehicle exhaust are still of priority to alleviate the VOC pollution. Apart from vehicle exhaust, the industrial emission was also an important VOC source at the JS and PD sites, the contributions of which herein were higher than those in other studies, except for Xi'an, China (29.7 %) and Paris, France (35 %). It is supported by locations of JS and PD sites i.e., the JS site is located at Second Jinshan Industrial Area of Shanghai as an industrial site, and Waigaoqiao Ship building LTD and BaoSteel Group Corporation are located within 30 km of the PD site, illustrating the great influence of industrial processes on VOC pollution at the both sites. However, limited influence of industrial source at the QP site was observed, which because the QP site is surrounded by natural environment and far away from the industrial regions. The discrepancies of combustion contribution also could be illustrated by the land-use types. In this case, the contribution of combustion was more pronounced at the JS site than the PD

and QP sites. As mentioned above, the JS site is surrounded by the industrial cluster and hence induced high emission of industrial combustion (Zhang et al., 2018). Moreover, the contribution of combustion varied greatly among different studies, from 4 % (Song et al., 2019b) to 46 % (Bari and Kindzierski, 2018) (Fig. 10), which was partially ascribed to the different definition of combustion. For instance, Song et al. (2019b) only regarded the wood combustion as the combustion source in the study of Seoul, South Korea, while the sum of fuel combustion and oil/natural gas extraction/combustion was summarized as combustion source in the study of Calgary, Canada (Bari and Kindzierski, 2018).

The contribution of fuel production and evaporation showed the obvious discrepancies among the different site locations. In detail, the contribution at the JS site (4.62 %) was lower than those in the previous studies (6.28-20 %), while it was relatively average at the PD site (10.35 %) (Li et al., 2018; Hui et al., 2018; Liu et al., 2019; Song et al., 2019a, b; Song et al., 2021). At the QP site, the result (20.15 %) was comparable with those from the other studies (11.65-20 %) (Hui et al., 2018; Liu et al., 2019; Song et al., 2019b; Gaimoz et al., 2011) (Fig. 10). The proportions of LPG usage were approximately twice higher at the sampling sites than those reported by the other studies (Hui et al., 2018; Song et al., 2019a). The fractions of paint solvent usage here were in the range of estimates by other cities (8.2-41 %) (Gaimoz et al., 2011; Bari and Kindzierski, 2018; Li et al., 2018; Liu et al., 2019; Hui et al., 2018; Song et al., 2019a, b; Liu et al., 2021; Song et al., 2021). The contribution of biomass burning at the QP site was relatively average compared to the estimates from other studies (Cai et al., 2010b; Gaimoz et al., 2011; Hui et al., 2018; Song et al., 2019 a, b) (Fig. 10). It is worth noting that VOC concentrations at the JS and PD sites were less influenced by the biomass burning relative to the QP site. Since the VOC concentrations were related to the emission strength and the mixing ratio of high intensity was determined by anthropogenic operation, it could be concluded that the human influences at the JS and PD sites were higher than that at the QP site which was consistent with the regional characteristics of anthrogopenic activities controlled by land-use types. Overall, the results of source contribution estimates varied with different studies (Lyu et al., 2016; Li et al., 2020b). The VOC sources also showed difference at a regional scale within the city (Tang et al., 2008; Li et al., 2019b; Cai et al., 2010; Song et al., 2021). These findings were particularly link to the land-use types, resulting in varying VOC species, sources, and emission strength (Li et al., 2019b; Cai et al., 2010; Li et al., 2020b; Song et al., 2021). Thus, the source apportionment for the different land-use types at a regional scale among various studies is necessary to identify the high-quality localized source.

4.3 The effect of land-use type on ozone and SOA formation potentials

The OFP values were closely related with the land-use types. In detail, the higher OFPs at the JS and PD sites (50.85 ± 2.63 and 33.94 ± 1.52 ppb) relative to that at the QP site (24.26 ± 1.43 ppb) were observed. Under the high OFPs, the concentrations of O_3 at the JS and PD sites (73.59 ± 23.59 and 57.48 ± 20.49 μg m^{-3}) were unexpectedly lower than that at the QP site (99.30 ± 24.00 μg m^{-3}), indicating the poor O_3 formation conditions, since the estimated OFP was proceeded under the optimum conditions. These results were due to the fact that the locations of JS and PD sites resulted in the high emission strength, which could release to high pollutant concentrations and lead to severe atmospheric pollution (Cai et al.,

2010a, b; Zhang et al., 2018). This phenomenon could change the strength of solar radiation and further decreased the intensity of photochemical reactions (Kumar et al., 2018). By contrast, the favorable meteorological conditions especially the intensive solar radiation at the QP site surrounded by vegetation were observed which contributed to the high O_3 concentration (Yoo et al., 2015). Such results were in good agreement with the findings in Zhengzhou, China (Li et al.,
625 2019b).

The discrepancies of SOAFP values among the sampling sites were observed since they could be significantly influenced by the land-use types. At the JS site, the SOAFP value (1.00 ± 2.03 μg m^{-3}) was 2.17 and 2.44 times higher than those at the PD (0.46 ± 0.88 μg m^{-3}) and QP (0.41 ± 0.58 μg m^{-3}) sites, which was consistent with variations of VOC concentrations especially aromatics and connected with the land-use types (Zhang et al., 2017; Jookjantra et al., 2022). The JS site is
630 surrounded by heavy industrial activities in paint and printing factory, manufacturing factory and rubber factory, resulting in the concentrated emission sources of industrial production (Zheng et al., 2010; An et al., 2014; Debevec et al., 2021). Because the close associations between VOCs and SOA could induce the sensitive response of VOC concentrations to the different pollution degree of PM$_{2.5}$, the VOCs-PM$_{2.5}$ sensitivity (VOCs-S$_{PM2.5}$) was applied to understand the plausible influence on the atmospheric PM$_{2.5}$ abundance. Atmospheric pollution here can be divided into five levels by the mass
635 concentration of PM$_{2.5}$: clean level (PM$_{2.5}$ < 35 μg m^{-3}), slight pollution level (35 < PM$_{2.5}$ < 75 μg m^{-3}), medium pollution level (75 < PM$_{2.5}$ < 120 μg m^{-3}), heavy pollution level (120 < PM$_{2.5}$ < 180 μg m^{-3}) and extreme pollution level (PM$_{2.5}$ > 180 μg m^{-3}) (Han et al., 2017). The variations of VOCs-S$_{PM2.5}$ as a function of PM$_{2.5}$ concentration at the JS, PD and QP sites are shown in Fig. 11. The low values of VOCs-S$_{PM2.5}$ basically remain constant, while the high values displayed a descending trend. In the clean level, VOCs-S$_{PM2.5}$ varied greatly from 0.19 to 2.50, 0.26 to 2.17 and 0.11 to 3.26 at the JS, PD and QP
640 sites, respectively. In the pollution level, the scope of VOCs-S$_{PM2.5}$ was narrow, especially in the extreme pollution level with the values fluctuating from 0.10 to 0.16, 0.13 to 0.17 and 0.17 to 0.28 at the JS, PD and QP sites, respectively. It is worth noting that the VOCs-S$_{PM2.5}$ values displayed a steady decreasing trend, and the ratios of PM$_{2.5}$ to $B_{PM2.5}$ increased in the clean and slight polluted levels. Such result demonstrated that the VOC concentrations were sensitive to that of PM$_{2.5}$ in the above two episodes. In order to quantify the sensitivity of VOCs to PM$_{2.5}$, we classified VOCs and PM$_{2.5}$ into different
645 groups with a PM$_{2.5}$ concentration interval of 5 μg m^{-3}, on the basis of the study reported by Han et al. (2017). The mean VOCs-S$_{PM2.5}$ values followed an exponential function, and the values of k were determined to be 0.39, 0.46 and 0.56 at the JS, PD and QP sites, respectively, according to the Eqs. (12-15). The VOCs at the QP site showed a more rapid increment along with the increase of PM$_{2.5}$ values. The four groups of VOCs displayed similar linkages with VOCs, and the higher values of k were attributed to the aromatics at the JS and PD sites, while the alkanes at the QP site (Fig. S5). Thus, the optimal choices
650 of controlling VOC species varied with the land-use types. Accordingly, in order to efficiently control the VOC-induced haze pollution, the concentrations of aromatics at the JS and PD sites, as well as alkanes at the QP site should be controlled in priority, as the results of the discrepancy of clean and haze day.

5. Conclusions

Herein, a concurrent atmospheric observation campaign was performed at the three supersites with the different land-use types of Shanghai from January to March 2019. Based on the observation data, this study carefully discussed the concentration variations, primary sources, ozone and SOA formation potentials of the atmospheric VOCs influenced by land-use types.

The VOC concentrations in the order of the JS (21.88 ± 12.58 ppb) > PD (21.36 ± 8.58 ppb) > QP (11.93 ± 6.33 ppb) sites were locally sensitive to the land-use types. Alkanes dominated the VOC community and accounted for 50.33, 71.48 and 60.88 % of the TVOCs at the JS, PD and QP sites, respectively because of their widespread emission sources and longer atmospheric lifetime. The relatively high VOC concentrations during the rush traffic hours in the morning and evening were observed at the sampling sites due to the vehicle emission. The "weekend effects" of VOCs showed that the VOC concentrations on the weekends were 3.31, 10.19 and 1.19 % lower than those on the weekdays at the JS, PD and QP sites, respectively, due to the low anthropogenic activities occurring on the weekends. Overall, the variations of VOC characteristics were closely related to the land-use types. The average $PM_{2.5}$ values were 45.57 ± 27.59, 48.51 ± 27.22 and 40.27 ± 27.78 μg m^{-3} at the JS, PD and QP sites, respectively. The highest O_3 concentration was observed at the QP site (99.30 ± 24.00 ppb), followed by the JS (73.59 ± 23.59 ppb) and PD (57.48 ± 20.49 ppb) sites. The occurrence of haze pollution was characterized by the elevated concentrations of aromatics at the JS and PD sites, while the alkanes at the QP site.

The special ratios and PMF were used to investigate the local sources. Local anthropogenic emissions contributed largely to the VOC pollution and varied with land-use types. The vehicle exhaust was determined as the predominate source at the three sites. The second largest VOC contributor was identified as industrial production at the JS and PD sites, whereas it proved to be the fuel production and evaporation at the QP site. The limited influence of industrial source at the QP site was observed which was related to the land-use type of this site i.e., the QP site is surrounded by natural environment and far away from the industrial regions. Relative to the QP site, JS and PD sites were less affected by the biomass burning which was consistent with the regional characteristics of anthrogopenic activities dominated by land-use types. Apart from the local sources, the influence of regional transport was analyzed *via* 24-h back trajectories and PSCF. The results showed that VOCs were impacted by the north or/and northeast trajectories at the sampling sites. The highest PSCF values were observed in the area near the above sites, indicating that local source was a significant contributor to the VOC pollution.

The formation potentials of O_3 and SOA induced by the studied VOCs were also discussed. During the observation period, relative to the SOA formation, the formation of O_3 was more dependent on the VOC concentrations, and the sensitivity analysis of VOC compositions varied with the land-use type. Specifically, the OFP results illustrated that alkenes were the major OFP contributor, and the aromatic compounds were also positively associated with the high OFP. The higher OFPs at the JS and PD sites (50.85 ± 2.63 and 33.94 ± 1.52 ppb) relative to that at the QP site (24.26 ± 1.43 ppb) were observed, while the O_3 concentrations were low. The result was related to the land-use types of both sites which led to high pollutant

concentrations and decreased the solar radiation and the intensity of photochemical reactions. In terms of SOAFP, BTEX was the greatest contributor to SOAFP, comprising 86.07, 96.21 and 86.38 % at the JS, PD and QP sites, respectively. The SOAFP values of each land-use types turned out to be in order of JS (1.00 ± 2.03 µg m^{-3}) > PD (0.46 ± 0.88 µg m^{-3}) > QP (0.41 ± 0.58 µg m^{-3}) sites, in connection with the land-use types. The VOCs-PM$_{2.5}$ sensitivity analysis showed that VOCs at

690   the QP site showed a more rapid increment along with the increase of PM$_{2.5}$ values compared with other two sampling sites. Of the four VOCs categories, aromatics at the JS and PD sites and alkanes at the QP site were more sensitive to PM$_{2.5}$. This finding indicated that alkenes and aromatics were key concerns in reducing the atmospheric secondary pollution in Shanghai. The relevant results herein reveal the influences of land-use type on atmospheric pollution, and set an example for the future VOC observation research at a city level.

Data availability

695

Measurement data in this study are available in the data repository maintained by Mendeley Data https://doi.org/10.17632/mf4gf36r9n.1 (Han, 2022).

Acknowledgements

700   This work was supported by National Key R&D Program of China (2022YFC3701102), National Natural Science Foundation of China (Nos. 22176038, 91744205, 21777025), and Natural Science Foundation of Shanghai City (22ZR1404700).

References

Ahmad, W., Coeur, C., Tomas, A., Fagniez, T., Brubach, J. B., and Cuisset, A.: Infrared spectroscopy of secondary organic aerosol precursors and investigation of the hygroscopicity of SOA formed from the OH reaction with guaiacol and syringol, Appl. Optics., 56(11), E116, https://doi.org/10.1364/AO.56.00E116, 2017.

Alghamdi, M. A., Khoder, M., Abdelmaksoud, A. S., Harrison, R. M., Hussein, T., Lihavainen, H., and Hämeri, K.: Seasonal and diurnal variations of BTEX and their potential for ozone formation in the urban background atmosphere of the coastal city Jeddah, Saudi Arabia, Air Qual. Atmos. Health 7(4), 467-480. https://doi.org/10.1007/s11869-014-0263-x, 2014.

Amor-Carro, O., White, K. M., Fraga-Iriso, R., Marinas-Pardo, L. A., Nunez-Naveira, L., Lema-Costa, B., Villarnovo, M., Verea-Hernando, H., and Ramos-Barbon, D.: Airway hyperresponsiveness, inflammation, and pulmonary emphysema in rodent models designed to mimic exposure to fuel oil-derived volatile organic compounds encountered during an experimental oil spill, Environ. Health Persp. 128: 027003, 1-14, https://doi.org/10.1289/EHP4178, 2020.

An, J., Zhu, B., Wang, H., Li, Y., Lin, X., and Yang, H.: Characteristics and source apportionment of VOCs measured in an industrial area of Nanjing, Yangtze River Delta, China, Atmos. Environ., 97, 206-214, https://doi.org/10.1016/j.atmosenv.2014.08.021, 2014.

An, J. L., Wang, J. X., Zhang, Y. X., and Zhu, B.: Source Apportionment of Volatile Organic Compounds in an Urban Environment at the Yangtze River Delta, China, Arch. Environ. Con. Tox., 72(3), 335-348, https://doi.org/10.1007/s00244-017-0371-3, 2017.

Ashbaugh, L. L., Malm, W. C., Sadeh, W. Z. A residence time probability analysis of sulfur concentrations at ground canyon national park, Atmos. Environ., 19(8), 1263-1270, https://doi.org/10.1016/0004-6981(85)90256-2, 1985.

Atkinson, R. and Arey, J: Gas-phase tropospheric chemistry of biogenic volatile organic compounds: a review, Atmos. Environ., 2, 37, https://doi.org/10.1016/S1352-2310(03)00391-1, 2003.

Bari, M. A. and Kindzierski, W. B.: Ambient volatile organic compounds (VOCs) in Calgary, Alberta: Sources and screening health risk assessment, Sci. Total Environ., 631-632, 627-640, https://doi.org/10.1016/j.scitotenv.2018.03.023, 2018.

Brown, S. G., Eberly, S., Paatero, P., Norris, and G. A.: Methods for estimating uncertainty in PMF solutions: Examples with ambient air and water quality data and guidance on reporting PMF results, Sci. Total Environ., 518-519, 626-635, https://doi.org/10.1016/j.scitotenv.2015.01.022, 2015.

Brown, S. G., Frankel, A., and Hafner, H. R.: Source apportionment of VOCs in the Los Angeles area using positive matrix factorization, Atmos. Environ., 41, 227-237, https://doi.org/10.1016/j.atmosenv.2006.08.021, 2007.

Cai, C., Geng, F., Yu, Q., An, J., Han, J.: Source apportionment of VOCs at city centre of Shanghai in summer, Acta Sci. Circumst., 30 (5), 926-934, https://doi.org/10.1631/jzus.A1000244, 2010a

Cai, C., Geng, F. H., Tie, X. X, Yu, Q., and An, J. L., Characteristics of ambient volatile organic compounds (VOCs) measured in Shanghai, China, Sensors, 10, 7843-7862, doi.:10.3390/s100807843, 2010b.

Calfapietra, C., Fares, S., and Lofeto, F: Volatile organic compounds from Italian vegetation and their interaction with ozone, Environ. Pollut., 157(5), 1478-1486, https://doi.org/10.1016/j.envpol.2008.09.048, 2009.

Carter, W. P. L.: Development of ozone reactivity scales for volatile organic compounds, J. Air Waste Manage. Assoc., 44(7), 881-899, https://doi.org/10.1080/1073161X.1994.10467290, 1994.

Chang, C. C., Wang, J. L., Liu, S. C., and Candice, L. S. C.: Assessment of vehicular and non-vehicular contributions to hydrocarbons using exclusive vehicular indicators, Atmos. Environ., 40, 6349-6361, https://doi.org/10.1016/j.atmosenv.2006.05.043, 2006.

Chen, C., Xia, Z. H., Wu, M. M., Zhang, Q. Q., Wnag, T., and Wang, L. P.: Concentrations, Source Identification, and Lung Cancer Risk Associated with Springtime $PM_{2.5}$-Bound Polycyclic Aromatic Hydrocarbons (PAHs) in Nanjing, China, Arch. Environ. Contam. Toxicol., 73, 391-400, https://doi.org/10.1007/s00244-017-0435-4, 2017.

Chen, T. M., Kuschner, W. G., Gokhale, J., and Schofer, S.: Outdoor air pollution: Ozone health effects, Am. J. Med. Sci., 333(4), 244-248, https://doi.org/10.1097/MAJ.0b013e31803b8e8c, 2007.

Chen, X., Millet, D. B., Singh, H. B., Wisthaler, A., Apel, E. C., Atlas, E. L., Blake, D. R., Bourgeois, I., Brown, S. S., Crounse, J. D., de Gouw, J. A., Flocke, F. M., Fried, A., Heikes, B. G., Hornbrook, R. S., Mikoviny, T., Min, K. E., Muller, M., Neuman, J. A., O'Sullivan, D. W., Peischl, J., Pfister, G. G., Richter, D., Roberts, J. M., Ryerson, T. B.,

Shertz, S. R., Thompson, C. R., Treadaway, V., Veres, P. R., Walega, J., Warneke, C., Washenfelder, R. A., Weibring, P., and Yuan, B: On the sources and sinks of atmospheric VOCs: an integrated analysis of recent aircraft campaigns over North Americ, Atmos. Chem. Phys., 19(14), 9097-9123, doi.:10.5194/acp-19-9097-2019, 2019.

Dai, H. X., Jing, S. G., Wang, H. L., Ma, Y. G., Li, L., Song, W. M., and Kan, H. D., VOC characteristics and inhalation health risks in newly renovated residences in Shanghai, China, Sci. Total Environ., 577, 73-83, https://doi.org/10.1016/j.scitotenv.2016.10.071, 2017.

Dai, P., Ge, Y., Lin, Y., Su, S., and Liang, B.: Investigation on characteristics of exhaust and evaporative emissions from passenger cars fueled with gasoline/methanol blends, Fuel. 2013, 113, 10-16, https://doi.org/10.1016/j.fuel.2013.05.038, 2013.

de Gouw, J. A., Middlebrook, A. M., Warneke, C., Ahmadov, R., Atlas, E. L., and Bahreini, R.: Organic aerosol formation downwind from the Deeperwater Horizon oil spil, Science 331, 1295-1299, https://doi.org/10.1126/science.1200320, 2011.

Debevec, C. Sauvage, S., Gros, V., Salameh, T. Sciare, J., Dulac, F., and Locoge, N.: Seasonal variation and origins of volatile organic compounds observed during 2 years at a western Mediterranean remote background site (Ersa, Cape Corsica), Atmos. Chem. Phys., 21, 1449-1484, https://doi.org/10.5194/acp-21-1449-2021, 2021.

Deng, C. X., Jin, Y. J., Zhang, M., Liu, X. W., and Yu, Z. M.: Emission Characteristics of VOCs from On-Road Vehicles in an Urban Tunnel in Eastern China and Predictions for 2017-2026, Aerosol Air Qual. Res., 18, 3025-3034, https://doi.org/10.4209/aaqr.2018.07.0248, 2018.

Draxier, R. R., and Hess, G. D.: An overview of the hysplit-4 modelling system for trajectories, Aust. Meteorol. Mag., 1998, 47(4), 295-308.

Dumanoglu, Y., Kara, M., Altiok, H., Odabasi, M., Elbir, T. and Bayram, A.: Spatial and seasonal variation and source apportionment of volatile organic compounds (VOCs) in a heavily industrialized region, Atmos. Environ., 98, 168-178, https://doi.org/10.1016/j.atmosenv.2014.08.048, 2014.

Gao, W., Tie, X., Xu, J., Huang, R., Mao, X., Zhou, G., and Chang, L.: Long-term trend of O_3 in a mega City 694 (Shanghai), China: Characteristics, causes, and interactions with precursors, Sci. Total Environ., 695 603-604, https://doi.org/10.1016/j.scitotenv.2017.06.099, 2017

Gaimoz, C., Sauvage, S., Gros, V., Herrmann, F., Williams, J., Locoge, N., Perrussel, O., Bonsang, B., d'Argouges, O., Sarda-Estève, R., and Sciare, J.: Volatile organic compounds sources in Paris in spring 2007. Part II: Source apportionment using positive matrix factorisation, Environ. Chem., 8, 91-103, https://doi.org/10.1071/EN10067, 2011.

Geng, F. H., Cai, C. J., Tie, X. X., Yu, Q., An, J. L., Peng, L., Zhou, G. Q., and Xu, J. M.: Analysis of VOC emissions using PCA/APCS receptor model at city of Shanghai, China, J. Atmos. Chem., 62(3), 229-247, https://doi.org/10.1007/s10874-010-9150-5, 2009.

Geng, F. H., Tie, X. X., Xu, J. M., Zhou, G. Q., Peng, L., Gao, W., Tang, X., and Zhao, C. S.: Characterizations of ozone, NOx, and VOCs measured in Shanghai, China, Atmos. Environ., 42, 6873-6883, doi.:0.1016/j.atmosenv.2008.05.045, 2008.

Grosjean, D. and Seinfeld, J. H.: Parameterization of the formation potential of secondary organic aerosols., Atmos. Environ., 23(8), 1733-1747, https://doi.org/10.1016/0004-6981(89)90058-9, 1989.

Gu, Y. X., Li, K., Xu, J. M., Liao, H., and Zhou, G. Q.: Observed dependence of surface ozone on increasing temperature in Shanghai, China, Atmos. Environ., 221, 117108, v https://doi.org/10.1016/j.atmosenv.2019.117108, 2020.

Guenther, A., Hewitt, C. N., Erickson, D., Fall, R., Geron, C., Graedel, T., Harley, P., Klinger, L., Lerdau, M., Mckay, W. A., Pierce, T., Scholes, B., Steinbrecher, R., Tallamraju, R., Taylor, J., and Zimmerman, P.: A global-model of natural volatile organic-compound emissions, J. Geophys. Res-A., 100, 8873-8892, https://doi.org/10.1029/94JD02950, 1995.

Guo, H., Cheng, H. R., Ling, Z. H., Louie, P. K. K., and Ayoko, G. A.: Which emission sources are responsible for the volatile organic compounds in the atmosphere of Pearl River Delta?, J. Hazard. Mater., 188(1-3), 116-124, https://doi.org/10.1016/j.jhazmat.2011.01.081, 2011.

Guo, H., Ling, Z. H., Cheng, H. R., Simpson, I. J., Lyu, X. P., Wang, X. M., Shao, M. Z., Lu, H. X., Ayoko, G., Zhang, Y. L., Saunders, S., Lam, S., Wang, J. L., and Blake, D. R.: Tropospheric volatile organic compounds in China, Sci. Total Environ., 574, 1021-1043, https://doi.org/10.1016/j.scitotenv.2016.09.116, 2017.

Guo, H., Wang, T., and Louie, P. K.: Source apportionment of ambient non-methane hydrocarbons in Hong Kong: application of a principal component analysis/absolute principal component scores (PCA/APCS) receptor model, Environ. Pollut., 129 (3), 489-498, https://doi.org/10.1016/j.envpol.2003.11.006, 2004.

Han, D. M., Wang, Z., Cheng, J. P., Wang, Q., Chen, X. J., and Wang, H. L.: Volatile organic compounds (VOCs) during non-haze and haze days in Shanghai: characterization and secondary organic aerosol (SOA) formation, Environ. Sci. Pollut. Res., 24, 18619-18629, https://doi.org/10.1007/s11356-017-9433-3, 2017.

Han, D. M., Gao, S., Fu, Q. Y., Cheng, J. P., Chen, X. J., Xu, H., Liang, S., Zhou, Y., and Ma, Y. N.: Do volatile organic compounds (VOCs) emitted from petrochemical industries affect regional $PM_{2.5}$? Atmos. Res., 209, 123-130, https://doi.org/10.1016/j.atmosres.2018.04.002, 2018.

Han, M., Lu, X. Q., Ran, L., Zhao, C. S., Han, S. Q., Bao, J. L., Zou, K. H., and Yan, F. Y.: Source apportionment of volatile organic compounds in urban Tianjin in the summer, Chin. Environ. Sci. Technol., 34(10), 76-80, https://doi.org/10.3969/j.issn.1003-6504.2011.10.017, 2011.

Han, Y.,: Data for: "Measurement report: Simultaneous multi-site observations of VOCs in Shanghai, East China: characteristics, sources and secondary formation potentials", Mendeley Data [data set], https://doi.org/10.17632/mf4gf36r9n.1, 2022.

He, Z. R., Wang, X. M., Ling, Z. H., Zhao, J., Guo, H., Shao, M., and Wang, Z.: Contributions of different anthropogenic volatile organic compound sources to ozone formation at a receptor site in the Pearl River Delta region and its policy implications, Atmos. Chem. Phys., 19(13), 8801-8816, https://doi.org/10.5194/acp-19-8801-2019, 2019.

Heald, C. L., Gouw, J. De, Goldstein, A. H., Guenther, A. B., Hayes, P. L., Hu, W., Isaacman-Vanwertz, G., Jimenez, J. L., Keutsch, F. N., Koss, A. R., Misztal, P. K., Rappenglück, B., Roberts, J. M., StevensP. S., Washenfelder, R. A., Warneke, C., and Young, C. J.: Contrasting reactive organic carbon observations in the Southeast United States (SOAS) and Southern California (CalNex), Environ. Sci. Technol., 54(23), 14923-14935, https://doi.org/10.1021/acs.est.0c05027, 2020.

Hennigan, C. J., Miracolo, M. A., Engelhart, G. J., May, A. A., Presto, A. A., Lee, T., Sullivan, A. P., Mucmeeking, G., Coe, H., Wold, C. E., Hao, W. M., Gilman, J. B., Kuster, W. C., Gouw, J. D., Schichtel, B., Collett-Jr, J. L., Kreidenweis, S. M., and Robinson, E. S.: Chemical and physical transformations of organic aerosol from the photo-oxidation of open biomass burning emissions in an environmental chamber, Atmos. Chem. Phys., 11, 7669-7686, https://doi.org/10.5194/acpd-11-11995-2011, 2011.

Hong, Z., Li, M., Wang, H., Xu, L., Hong, Y., Chen, J., Chen, J., Zhang, H., Zhang, Y., Wu, X., Hu, B., and Li, M.: Characteristics of atmospheric volatile organic compounds (VOCs) at a mountainous forest site and two urban sites in the southeast of China, Sci. Total Environ., 657, 1491-1500, https://doi.org/10.1016/j.scitotenv.2018.12.132, 2019.

Hoshi, J., Amano, S., Sasaki, Y., and Korenaga, T.: Investigation and estimation of emission sources of 54 volatile organic compounds in ambient air in Tokyo, Atmos. Environ., 42(10), 2383-2393, https://doi.org/10.1016/j.atmosenv.2007.12.024, 2008.

Hopke, P. K. Review of receptor modeling methods for source apportionment, J. Air Waste Manage. Assoc., 66(3), 237-259, https://doi.org/10.1080/10962247.2016.1140693, 2016.

Huang, C., Wang, H. L., Li, L., Wang, Q., Lu, Q., de Gouw, J. A., Zhou, M., Jing, S. A., Lu, J., and Chen, C. H.: VOC species and emission inventory from vehicles and their SOA formation potentials estimation in Shanghai, China, Atmos. Chem. Phys., 15, 11081-11096, https://doi.org/10.5194/acp-15-11081-2015, 2015.

Huang, R. J., Zhang, Y., Bozzetti, C., Ho, K. F., Cao, J. J., Han, Y. M., Daellenbach, K. R., Slowik, J. G., Platt, S. M., Canonaco, F., Zotter, P., Wolf, R., Pieber, S. M., Bruns, E. A., Crippa, M., Ciarelli, G., Piazzalunga, A., Schwikowski, M., Abbaszade, G., Schnelle-Kreis, J., Zimmermann, R., An, Z., Szidat, S., Baltensperger, U., Haddad, I. E., and Prévôt, A. S. H.: High secondary aerosol contribution to particulate pollution during haze events in China, Nature, 514, 218-222, https://doi.org/10.1038/nature13774, 2014.

Hui, L. R., Liu, X. G., Tan, Q. W., Feng, M., An, J. L., Qu, Y., Zhang Y. H., and Cheng, N. L.: VOC characteristics, sources and contributions to SOA formation during haze events in Wuhan, Central China, Sci. Total Environ., 650, 2624-2639, https://doi.org/10.1016/j.scitotenv.2018.10.029, 2019.

Hui, L. R., Liu, X. G., Tan, Q. W., Feng, M., An, J. L., Qu, Y., Zhang, Y. H., and Jiang, M. Q.: Characteristics, source apportionment and contribution of VOCs to ozone formation in Wuhan, Central China, Atmos. Environ., 192, 55-71, https://doi.org/10.1016/j.atmosenv.2018.08.042, 2018.

Jobson, B. T., Parrish, D. D., Goldan, P., Kuster, W., Fehsenfeld, F. C., Blake, D. R., and Niki, H.: Spatial and temporal variability of nonmethane hydrocarbon mixing ratios and their relation to photochemical lifetime, J. Geophys. Res. Atmos., 103(D11), 13557-13567, https://doi.org/10.1029/97JD01715, 1998.

Jookjantra, P., Thepanondh, S., Keawboonchu, J., Kultan, V., and Laowagul, W.: Formation potential and source contribution of secondary organic aerosol from volatile organic compounds, J. Environ. Qual., 1-40, https://doi.org/10.1002/jeq2.20381, 2022.

Kuo, C. P., Liao, H. T., Chou, C. C. K., and Wu, C. F.: Source apportionment of particulate matter and selected volatile organic compounds with multiple time resolution data, Sci. Total Environ., 472, 880-887, http://dx.doi.org/10.1016/j.scitotenv.2013.11.114, 2014.

Kumar, A., Singh, D., Kumar, K. S., Singh, B. B., and Jain, V. K.: Distribution of VOCs in urban and rural atmospheres of subtropical India: Temporal variation, source attribution, ratios, OFP and risk assessment, Sci. Total Environ., 613-614, 492-501, https://doi.org/10.1016/j.scitotenv.2017.09.096, 2018.

Lai, C., Chuang, K., and Chang, J.: Source apportionment of volatile organic compounds at an international airport, Aerosol Air Qual. Res., 13, 689-698, https://doi.org/10.4209/aaqr.2012.05.0121, 2013.

Lam, S. H. M., Saunders, S. M., Guo, H., Ling, Z. H., Jiang, F., Wang, X. M., and Wang, T. J.: Modelling VOC source impacts on high ozone episode days observed at a mountain summit in Hong Kong under the influence of mountain-valley breezes, Atmos. Environ., 81(2), 166-176, https://doi.org/10.1016/j.atmosenv.2013.08.060, 2013.

Li, B., Ho, S. S. H., Gong, S., Ni, J., Li, H., Han, L., Yang, Y., Qi, Y., and Zhao, D.: Characterization of VOCs and their related atmospheric processes in a central Chinese city during severe ozone pollution period, Atmos. Chem. Phys., 9(1), 617-638, https://doi.org/10.5194/acp-19-617-2019, 2019b.

Li, J., Xie, S. D., Zeng, L. M., Li, L. Y., Li, Y. Q., and Wu, R. R.: Characterization of ambient volatile organic compounds and their sources in Beijing, before, during, and after Asia-Pacific Economic Cooperation China 2014, Atmos. Chem. Phys., 15(14), 7945-7959, https://doi.org/ 10.5194/acp-15-7945-2015, 2015a.

Li, J., Zhai, C. Z., Yu, J. Y., Liu, R. L., Li, Y. Q., Zeng, L. M., and Xie, S. D.: Spatiotemporal variations of ambient volatile organic compounds and their sources in Chongqing, a mountainous megacity in China, Sci. Total Environ., 627, 1442-1452, https://doi.org/10.1016/j.scitotenv.2018.02.010, 2018.

Li, L., Tan, Q., Zhang, Y., Feng, M., Qu, Y., An, J., and Liu, X.: Characteristics and source apportionment of $PM_{2.5}$ during persistent extreme haze events in Chengdu, Southwest China, Environ. Pollut., 230, 718-729, https://doi.org/10.1016/j.envpol.2017.07.029, 2017.

Li, L., Xie, S., Zeng, L., Wu, R., and Li, J.: Characteristics of volatile organic compounds and their role in ground-level ozone formation in the Beijing-Tianjin-Hebei region, China, Atmos. Environ., 113, 247-254, https://doi.org/10.1016/j.atmosenv.2015.05.021, 2015b.

Li, M., Zhang, Q., Zheng, B., Tong, D., Lei, Y., Liu, F., Hong, C., Kang, S., Yan, L., Zhang, Y., Bo, Y., Su, H., Cheng, Y., and He, K.: Persistent growth of anthropogenic non-methane volatile organic compound (NMVOC) emissions in China during 1990-2017: drivers, speciation and ozone formation potemtial, Atmos. Chem. Phys., 19, 8897-8913, https://doi.org/10.5194/acp-19-8897-2019, 2019c.

Li, X. H., Wang, S. X., and Hao, J. M.: Characteristics of Volatile Organic Compounds (VOCs) Emitted from Biofuel Combustion in China, Environ, Sci., 32, 3515-3521, https://doi.org/10.1109/ICMTMA.2014.201, 2011.

Li, X. L., Iida, A., Liu, J. F., Bao, L. M., Li, Y., and Zhang, G. L.: Source identification of individual $PM_{2.5}$ particles in Shanghai air in the winter of 2007 with synchrotron X-ray fluorescence microprobe, Chinese Phys. C., 33(11): 960-964, https://doi.org/10.1088/1674-1137/33/11/006, 2009.

Li, Y. D., Yin, S. S., Yu, S. J., Yuan, M. H., Dong, Z., Zhang, D., Yang, L. M., and Zhang, R. Q.: Characteristics, source apportionment and health risks of ambient VOCs during high ozone period at an urban site in central plain, China, Chemosphere, 250, 126283, https://doi.org/10.1016/j.chemosphere.2020.126283, 2020a.

Li, Y. J., Ren, B. N., Qiao, Z., Zhu, J. P., Wang, H. L., Zhou, M., Qiao, L. P., Lou, S. R., Jing, S. G., Huang, C., Tao, S. K., Rao, P. H., and Li, J.: Characteristics of atmospheric intermediate volatility organic compounds (IVOCs) in winter and summer under different air pollution levels, Atmos. Environ., 210, 58-65, https://doi.org/10.1016/j.atmosenv.2019.04.041, 2019a.

Li, Z. Y., Ho, K. F., and Yin, S. H. L.: Source apportionment of hourly-resolved ambient volatile organic compounds: Influence of temporal resolution, Sci. Total Environ., 725, 138243, https://doi.org/10.1016/j.scitotenv.2020.138243, 2020b.

Lim, Y. B., Tan, Y., Perri, M. J., Seitzinger, S. P., and Turpin, B. J.: Aqueous chemistry and its role in secondary organic aerosol (SOA) formation, Atmos. Chem. Phys., 10, 14161-14207, https://doi.org/10.5194/acpd-10-14161-2010, 2010.

Ling, Z. H., Guo, H., Cheng, H. R., and Yu, Y. F.: Sources of ambient volatile organic compounds and their contributions to photochemical ozone formation at a site in the Pearl River Delta, southern China, Environ. Pollut., 159 (10), 2310-2319, https://doi.org/10.1016/j.envpol.2011.05.001, 2011.

Liu, J., Chu, B. W., Jia, Y. C., Cao, Q., Zhang, H., Chen, T. Z., Ma, Q. X., Ma, J. Z., Wang, Y. H., Zhang, P., and Hong, H.: Dramatic decrease of secondary organic aerosol formation potential in Beijing: Important contribution from reduction of coal combustion emission, Sci. Total Environ., 832, 155045, http://dx.doi.org/10.1016/j.scitotenv.2022.155045, 2022.

Liu, S. C.: Ozone production in the rural troposphere and the implications for regional and global ozone distributions., J. Geophys. Res., 92(D4), 4191-4207, https://doi.org/10.1029/JD092iD04p04191, 1987.

Liu, Y., Shao, M., Fu, L. L., Lu, S. H., Zeng, L. M., and Tang, D. G.: Source profiles of volatile organic compounds (VOCs) measured in China: Part I, Atmos. Environ., 42(25), 6247-6260. https://doi.org/10.1016/j.atmosenv, 2008.

Liu, Y., Song, M., Liu, X., Zhang, Y., Hui, L., Kong, L., Zhang, Y., Zhang, C., Qu, Y., An, J., Ma, D., Tan, Q., and Feng, M.: Characterization and sources of volatile organic compounds (VOCs) and their related changes during ozone pollution days in 2016 in Beijing, China, Environ. Pollut., 257, 113599, 1-12, https://doi.org/10.1016/j.envpol.2019.113599, 2020.

Liu, Y., Wang, H., Jing, S., Gao, Y., Peng, Y., Lou, S., Cheng, T., Tao, S., Li, L., Li, Y., Huang, D., Wang, Q., and An, J.: Characteristics and sources of volatile organic compounds (VOCs) in Shanghai during summer: Implications of regional transport, Atmos. Environ., 215, 116902, 1-14, https://doi.org/10.1016/j.atmosenv.2019.116902, 2019.

Liu, Y. H., Wang, H. L., Jing, S. G., Peng, Y. R., Gao, Y. Q., Yan, R. S., Wang, Q., Lou, S. R., Cheng, T. T., and Huang, C.: Strong regional transport of volatile organic compounds (VOCs) during wintertime in Shanghai megacity of China, Atmos. Environ., 244, 117940, https://doi.org/10.1016/j.atmosenv.2020.117940, 2021.

Lu, X., Hong, J., Zhang, L., Cooper, O. R., Schultz, M. G., Xu, X., Wang, T., Gao, M., Zhao, Y., and Zhang, Y.: Severe surface ozone pollution in China: A global perspective, Environ. Sci. Technol. Lett., 5, 487-494, https://doi.org/10.1021/acs.estlett.8b00366, 2018.

Lyu, X. P., Chen, N., Guo, H., Zhang, W. H., Wang, N., Wang, Y., and Liu, M.: Ambient volatile organic compounds and their effect on ozone production in Wuhan, Central China, Sci. Total Environ., 541, 662-669, https://doi.org/10.1016/j.scitotenv.2015.09.093, 2016.

Ma, T., Duan, F., He, K., Qin, Y., Tong, D., Geng, G., Liu, X., Li, H., Yang, S., Ye, S., Xu, B., Zhang, Q., and Ma, Y.: Air pollution characteristics and their relationship with emissions and meteorology in the Yangtze River Delta region during 2014-2016, J. Environ. Sci., 83, 8-20, https://doi.org/10.1016/j.jes.2019.02.031, 2019.

Merikanto, J., Spracklen, D. V., Mann, G. W., Pickering, S. J., and Carslaw, K. S.:Impact Impact of nucleation on global CCN, Atmos. Chem. Phys., 9, 8601-8616, https://doi.org/10.5194/acp-9-8601-2009, 2009.

Mo, Z., Shao, M., Lu, S., Qu, H., Zhou, M., Sun, J., and Gou, B.: Process-specific emission characteristics of volatile organic compounds (VOCs) from petrochemical facilities in the Yangtze River Delta, China, Sci. Total Environ., 533, 422-431, https://doi.org/10.1016/j.scitotenv.2015.06.089, 2015.

Mo, Z., Shao, M., Lu, S.: Compilation of a source profile database for hydrocarbon and OVOC emissions in China, Atmos. Environ., 143, 209-217, https://doi.org/10.1016/j.atmosenv.2016.08.025, 2016.

Monod, A., Sive, B. C., Avino, P., Chen, T., Blake, D. R., and Rowland, F. S.: Monoaromatic compounds in ambient air of various cities: a focus on correlations between the xylenes and ethylbenzene, Atmos. Environ., 35, 135-149, https://doi.org/10.1016/S1352-2310(00)00274-0, 2001.

Mousavinezhad, S., Choi, Y., Pouyaei, A., Ghahremanloo, M. and Nelson, D. L.: A comprehensive investigation of surface ozone pollution in China, 2015-2019: Separating the contributions from meteorology and precursor emissions, Atmos. Res., 257, 105599, https://doi.org/10.1016/j.atmosres.2021.105599, 2021.

Morrow, N.L.: The industrial production and use of 1,3-butadiene, Environ. Health Perspect., 86, 7-8, https://doi.org/10.1289/ehp.90867, 1990.

Mozaffar, A., Zhang, Y. L., Fan, M. Y., Cao, F., and Lin, Y. C.: Characteristics of summertime ambient VOCs and their contributions to O_3 and SOA formation in a suburban area of Nanjing, China, Atmos. Res., 240, 104923, 1-16, https://doi.org/10.1016/j.atmosres.2020.104923, 2020.

Murphy, J. G., Day, D. A., Cleary, P. A., Wooldridge, P. J., Millet, D. B., Goldstein, A. H., and Cohen, R. C.: The weekend effect within and downwind of Sacramento-Part 1: Observation of ozone, nitrogen oxides, and VOC reactivity, Atmos. Chem. Phys., 7(20): 5237-5339, https://doi.org/10.5194/acp-7-5327-2007, 2007.

Nan, S. Q., Liang, J., Zhang, D., Zhang, R. Q., Jiang, N., Duo, K. X., and Zhang, J.: VOCs in ambient air of Zhengzhou City: spatial distribution and source apportionment, China Environ. Sci. Technol., 38(3), 119-124, https://doi.org/10.3969/j.issn.1003-6504.2015.03.023, 2015.

Nelson, P., and Quigley, S.: The m, p-xylenes: ethylbenzene ratio. A technique for estimating hydrocarbon age in ambient atmospheres, Atmos. Environ., 17, 659-662,
https://doi.org/10.1016/0004-6981(83)90141-5, 1983.

Ng, N. L., Kroll, J. H., Chan, A. W. H., Chhabra, P. S. Flagan, R. C., and Seinfeld, J. H.: Secondary organic aerosol formation from m-xylene, toluene, and benzene, Atmos. Chem. Phys., 7(14), 3909-3922, https://doi.org/10.5194/acp-7-3909-2007, 2007.

Niu, H., Mo, Z., Shao, M., Lu, S., and Xie, S.: Screening the emission sources of volatile organic compounds (VOCs) in China by multi-effects evaluation, Front. Env. Sci. Eng., 10(5), 1-11, https://doi.org/10.1007/s11783-016-0828-z, 2016.

Nussbaumer, C. M. and Cohen, R. C.: The role of temperature and NOx in ozone trends in the Los Angeles Basin, Environ. Sci. Technol., 54, 15652-15659, https://doi.org/10.1021/acs.est.0c04910, 2020.

Odum, J. R., Jungkamp, T. P. W., Griffin, R. J., Forstner, H. J. L., Flagan, R. C., and Seinfeld, J. H.: Aromatics, reformulated gasoline, and atmospheric organic aerosol formation, Environ. Sci. Technol., 31(7), 1890-1897, https://doi.org/10.1021/es960535l, 1997.

Ou, J., Yuan, Z., Zheng, J., Huang, Z., Shao, M., Li, Z., Huang, X., Guo, H., and Louie, P. K.: Ambient Ozone 810 Control in a Photochemically Active Region: Short-Term Despiking or Long-Term Attainment?, Environ. Sci. Tech., 50, 5720-5728, https://doi.org/10.1021/acs.est.6b00345, 2016.

Paatero, P.: Least squares formulation of robust non-negative factor analysis, Chemom. Intell. Lab. Syst., 37(1), 23-35, https://doi.org/10.1016/S0169-7439(96)00044-5, 1997.

Pakkattil, A., Muhsin, M., and Varma, M. K. R: COVID-19 lockdown: Effect on selected volatile organic compound (VOC) emissions over the major Indian metro cities, 37, 100838, https://doi.org/10.1016/j.uclim.2021.100838, 2021.

Pallavi, Sinha, B., and Sinha, V.: Source apportionment of volatile organic compounds in the northwest Indo-Gangetic Plain using a positive matrix factorization model, Atmos. Chem. Phys., 19(24), 15467-15482, https://doi.org/10.5194/acp-19-15467-2019, 2019.

Pankow, J. F.: An absorption-model of gas-particle partitioning of organic-compounds in the atmosphere, Atmos. Environ., 28, 185-188, https://doi.org/10.1016/1352-2310(94)90093-0, 1994.

Polissar, A. V., Hopke, P. K., Paatero, P., Kaufmann, Y. J., Hall, D. K., Bodhaine, B. A., Dutton, E. G., and Harris, J. M.: The aerosol at Barrow, Alaska: long-term trends and source locations, Atmos. Environ., 33, 2441-2458, https://doi.org/10.1016/S1352-2310(98)00423-3, 1999.

Qin, G. M., Gao, S., Fu, Q. Y., Fu, S., Jia, H. H., Zeng, Q. R., Fan, L. P., Ren, H. R., and Cheng, J. P.: Investigation of VOC characteristics, source analysis, and chemical conversions in a typical petrochemical area through 1-year monitoring and emission inventory, Environ. Sci. Pollut. R., 29(34), 51635-51650, https://doi.org/10.1007/s11356-022-19145-7, 2022.

Ren, B. N., Zhu, J. P., Tian, L. J., Wang, H. L., Huang, C., Jing, S. A., Lou, S. G., An, J. Y., Lu, J., Rao, P. H., Fu, Q. Y., Huo, J. T., and Li, Y. J.: An alternative semi-quantitative GC/MS method to estimate levels of airborne intermediate volatile organic compounds (IVOCs) in ambient air, Atmos. Environ., 6, 100075, https://doi.org/10.1016/j.aeaoa.2020.100075, 2020.

Rumchev, K., Brown, H., and Spickett, J.: Volatile organic compounds: do they present a risk to our health?, Rev. Environ. Health, 22(1), 39-55, https://doi.org/10.1515/REVEH.2007.22.1.39, 2007.

Sadeghi, B., Pouyaei, A., Choi, Y. S., and Rappenglueck, B. H.: Measurement report: Summertime and wintertime VOCs in Houston: Source apportionment and spatial distribution of source origins, Atmos. Chem. Phys. Discussion, 2021, 565, 1-27, https://doi.org/10.5194/acp-2021-565, 2021.

Sawvel, E. J., Willis, R., West, R. R., Casuccio, G. S., Norris, G., Kumar, N., Hammond, D., and Peters, T. M.: Passive sampling to capture the spatial variability of coarse particles by composition in Cleveland, OH, Atmos. Environ., 105, 61-69, https://doi.org/10.1016/j.atmosenv.2015.01.030, 2015.

Seinfeld, J. H., Erdakos, G. B., Asher, W. E., and Pankow, J. F.: Modeling the formation of secondary organic aerosol (SOA). 2. The predicted effects of relative humidity on aerosol formation in the α-pinene-, β-pinene-, sabinene-, Δ3-carene-, and cyclohexene-ozone systems. Environ. Sci. Technol., 35, 1806-1817, https://doi.org/10.1021/es011025g, 2001.

Schauer, J. J., Kleeman, M. J., Cass, G. R., and Simoneit, B. R. T.: Measurement of emissions from air pollution sources. 3. C-1-C-29 organic compounds from fireplace combustion of wood, Environ. Sci. Technol., 35, 1716e1728, https://doi.org/10.1021/es001331e, 2001.

Schwantes, R. H., Schilling, K. A., Mcvay, R. C., Lignell, H., and Seinfeld, J. H.: Formation of highly oxygenated low-volatility products from cresol oxidation, Atmos. Chem. Phys., 17(5), 1-34, https://doi.org/10.5194/acp-17-3453-2017, 2016.

Shao, M., Lu, S., Liu, Y., Xie, X., Chang, C., Huang, S., and Chen, Z.: Volatile organic compounds measured in summer in Beijing and their role in ground-level ozone formation, J. Geophys. Res, 114, 833, https://doi.org/10.1029/2008jd010863, 2009.

Shao, P., An, J. L., Xin, J. Y., Wu, F. K., Wang, J. X., Ji, D. S., and Wang, Y. S.: Source apportionment of VOCs and the contribution to photochemical ozone formation during summer in the typical industrial area in the Yangtze River Delta, China, Atmos. Res., s176-s177, 64-74, https://doi.org/10.1016/j.atmosres.2016.02.015, 2016.

Shi, C. Z., Wang, S., Liu, R., Zhou, R., Li, D., Wang, W., Li, Z., Cheng, T., and Zhou, B.: A study of aerosol optical properties during ozone pollution episodes in 2013 over Shanghai, China, Atmos. Res, 153, 235-249, https://doi.org/10.1016/j.atmosres.2014.09.002, 2015.

Shi, J., Deng, H., Bai, Z., Kong, S., Wang, X., Hao, J., Han, X., and Ning, P.: Emission and profifile characteristic of volatile organic compounds emitted from coke production, iron smelt, heating station and power plant in Liaoning Province, China, Sci. Total Environ., 515, 101-108, https://doi.org/10.1016/j.scitotenv.2015.02.034, 2015.

Sjostedt, S. J., Slowik, J. G., Brook, J. R., Chang, Y. W., Mihele, C., Stroud, C. A., Vlasenko, A., and Abbatt, J. P. D.: Diurnally resolved particulate and VOC measurements at a rural site: indication of significant biogenic secondary organic aerosol formation, Atmos. Chem. Phys., 11, 5745-5760, https://doi.org/10.5194/acp-11-5745-2011, 2011.

Song, C. B., Wu, L., Xie, Y. C., He, J. J., Chen, X., Wang, T., Lin, Y. C., Jin, T. S., Wang, A. X., Liu, Y., Dai, Q. L., Liu, B. S., Wang, Y. N., and Mao, H. J.: Air pollution in China: Status and spatiotemporal variations, Environ. Pollut., 227, 334-347, https://doi.org/10.1016/j.envpol.2017.04.075, 2017.

Song, M., Tan, Q., Feng, M., Qu, Y., Liu, X., An, J. and Zhang, Y.: Source Apportionment and Secondary Transformation of Atmospheric Nonmethane Hydrocarbons in Chengdu, Southwest China, J. Geophys. Res. Atmos., 123(17), 9741-9763, https://doi.org/10.1029/2018JD028479, 2018.

Song, M. D., Li, X., Yang, S. D., Yu, X. N., Zhou, S. X., Yang, Y. M., Chen, S. Y., Dong, H. B., Liao, K. R., Chen, Q., Lu, K. D., Zhang, N. N., Cao, J. J., Zeng, L. M., and Zhang, Y. H.: Spatiotemporal variation, sources, and secondary transformation potential of volatile organic compounds in Xi'an China, Atmos. Chem. Phys., 21, 4939-4958, https://doi.org/10.5194/acp-21-4939-2021, 2021.

Song, M. D., Liu, X.G., Zhang, Y.H., Shao, M., Lu, K.D., Tan, Q.W., Feng, M. and Qu, Y.: Sources and abatement mechanisms of VOCs in southern China, Atmos. Environ., 201, 28-40, https://doi.org/10.1016/j.atmosenv.2018.12.019, 2019a.

Song, S. K., Shon, Z. H., Kang, Y. H., Kim, K. H., Han, S. B., Kang, M. S., Bang, J. H., and Oh, I.: Source apportionment of VOCs and their impact on air quality and health in the megacity of Seoul, Environ. Pollut., 247, 763-774, https://doi.org/10.1016/j.envpol.2019.01.102, 2019b.

Song, Y., Shao, M., Liu, Y., Lu, S., Kuster, W., Goldan, P., and Xie, S.: Source apportionment of ambient volatile organic compounds in Beijing, Environ. Sci. Technol., 41(12), 4348-4353, https://doi.org/10.1021/es0625982, 2007.

Spracklen, D. V., Jimenez, J. L., Carslaw, K. S., Worsnop, D. R., Evans, M. J., Mann, G. W., Zhang, Q., Canagaratna, M. R., Allan, J., Coe, H., McFiggans, G., Rap, A., and Forster, P.: Aerosol mass spectrometer constraint on the global secondary organic aerosol budget, Atmos. Chem. Phys., 11, 12109-12136, https://doi.org/10.5194/acp-11-12109-2011, 2011.\

Sun, J., Wu, F. K., Hu, B., Tang, G. Q., Zhang, J. K., and Wang, Y. S.: VOC characteristics, emissions and contributions to SOA formation during haze episodes, Atmos. Environ., 141, 560-570, https://doi.org/10.1016/j.atmosenv.2016.06.060, 2016.

Tan, Z., Lu, K., Jiang, M., Su, R., Dong, H., Zeng, L., Xie, S. D., Tan, Q. W., and Zhang, Y. H.: Exploring ozone pollution in Chengdu, southwestern China: A case study from radical chemistry to O_3-VOC-NO_x sensitivity, Sci. Total Environ., 636, 775-786, https://doi.org/10.1016/j.scitotenv.2018.04.286, 2018.

Tang, J. H., Chan, L. Y., Chan, C. Y., Li, Y. S., Chang, C. C., Wang, X. M., and Wu, D.: Implications of changing urban and rural emissions on non-methane hydrocarbons in the Pearl River Delta region of China. Atmos. Environ., 42 (16), 3780-3794, https://doi.org/10.1016/j.atmosenv.2007.12.069, 2008.

Tian, L., Li, Y. F., Shao, L., and Zhang, Y.: Measuring Spatio-temporal Characteristics of City Expansion and Its Driving Forces in Shanghai from 1990 to 2015, Chin. Geogra. Sci., 27, 875-890, https://doi.org/10.1007/s11769-017-0883-9, 2017.

Tie, X., Geng, F., Guenther, A., Gao, J., Greenberg, J., Zhang, R., Apel, E., Lil, G., Weinheimer, A., Chen, J., and Cai, C.: Megacity impacts on regional ozone formation: observations and WRF-Chem modeling for the MIRAGE-Shanghai field campaign, Atmos. Chem. Phys.,13, 5655-5669, https://doi.org/10.5194/acp-13-5655-2013, 2013.

Toro, R., Seguel, R. J., Morales, R. G. E., and Leiva, M. A: Ozone, nitrogen oxides, and volatile organic compounds in a central zone of Chile, Air Qual. Atmos. Hlth., 8(6), 545-557, https://doi.org/10.1007/s11869-014-0306-3, 2015.

US EPA: Photochemical Assessment Monitoring Stations (PAMS), available at: http://www3.epa.gov/ttnamti1/pamsmain.html, 1990.

Vardoulakis, S., Solazzo, E., and Lumbreras, J.: Intra-urban and street scale variability of BTEX, NO2 and O_3 in Birmingham, UK: Implications for exposure assessment, Atmos. Environ., 45(29), 5069-5078, https://doi.org/10.1016/j.atmosenv.2011.06.038, 2011.

Velasco, E., Lamb, B., Westberg, H., Allwine, E., Sosa, G., Arriaga-Colina, J. L., Jobson, B. T., Alexander, M. L., Prazeller, P., Knighton, W. B., Rogers, T. M., Grutter, M., Herndon, S. C., Kolb, C. E., Zavala, M., de Foy, B., Volkamer, R., Molina, L. T., and Molina, M. J.: Distribution, magnitudes, reactivities, ratios and diurnal patterns of volatile organic compounds in the Valley of Mexico during the MCMA 2002&2003 field campaigns, Atmos. Chem. Phys., 7, 329-353, https://doi.org/10.5194/acp-7-329-2007, 2007.

von Schneidemesser, E., Monks, P. S., and Plass-Duelmer, C.: Global comparison of VOC and CO observations in urban areas, Atmos. Environ., 44(39), 5053-5064, https://doi.org/10.1016/j.atmosenv.2010.09.010, 2010.

Vo, T. D. H., Lin, C. S., Weng, C. E., Yuan, C. S., Lee, C. W., Hung, C. H., Bui, X. T., Lo, K. C., and Lin, J. X.: Vertical stratification of volatile organic compounds and their photochemical product formation potential in an industrial area, J. Environ. Manag., 217, 327-336, doi.:10.1016/j.jenvman.2018.03.101, 2018.

Wang, H. L., Gao, Y. Q., Jing, S. A., Lou, S. R., Hu, Q. Y., An, J. Y., Wu, Y. H., Gao, W., Zhu, L., and Huang, C.: Characterization of volatile organic compounds (VOCs) using mobile monitoring around the industrial parks in the Yangzte River Delta region of China, Huan jing ke xue= Huanjing kexue / [bian ji, Zhongguo ke xue yuan huan jing ke xue wei yuan hui Huan jing ke xue bian ji wei yuan hui, 42(3), 1298-1305, https://doi.org/10.13227/j.hjkx.202007265, 2021.

Wang, J., Hu, Z. M., Chen, Y. Y., Chen, Z. L., Xu, and S. Y.: Contamination characteristics and possible sources of PM10 and $PM_{2.5}$ in different functional areas of Shanghai, China, Sci. Total Environ., 68, 221-229, https://doi.org/10.1016/j.atmosenv.2012.10.070, 2013.

Wang, M., Shao, M., Lu, S. H., Yang, Y. D., and Chen, W. T.: Evidence of coal combustion contribution to ambient VOCs during winter in Beijing, Chin. Chem. Lett., 24(9), 829-832, https://doi.org/10.1016/j.cclet.2013.05.029, 2013.

Wang, P., Chen, Y., Hu, J. L., Zhang, H. L., and Ying, Q.: Source apportionment of summertime ozone in China using a sourceoriented chemical transport model, Atmos. Environ., 211, 79-90, https://doi.org/10.1016/j.atmosenv.2019.05.006, 2019.

Wang, P., Wang, T., and Ying, Q.: Regional source apportionment of summertime ozone and its precursors in the megacities of Beijing and Shanghai using a source-oriented chemical transport model, Atmos. Environ., 224, 117337, https://doi.org/10.1016/j.atmosenv.2020.117337, 2020.

Wang, Q., Liu, M., Yu, Y. P., and Li, Y.: Characterization and source apportionment of $PM_{2.5}$-bound polycyclic aromatic hydrocarbons from Shanghai city, China, Environ. Pollu., 218, 118-128, https://doi.org/10.1016/j.envpol.2016.08.037, 2016.

Wang, R., Xu, X. B., Jia, S. H., Ma, R. S., Ran, L., Deng, Z. Z., Lin, W. L., Wang, Y., and Ma, Z. Q: Lower tropospheric distributions of O_3 and aerosol over Raoyang, a rural site in the North China Plain, Atmos. Chem. Phys., 17, 3891-3903, https://doi.org/10.5194/acp-17-3891-2017, 2017.

Wang, T., Xia, Z. H., Wu, M. M., Zhang, Q. Q., Sun, S. Q., Yin, J., Zhou, Y. C., and Yang, H.: Pollution characteristics, sources and lung cancer risk of atmospheric polycyclic aromatic hydrocarbons in a new urban district of Nanjing, China, J. Environ. Sci., 55, 118-128, https://doi.org/10.1016/j.jes.2016.06.025, 2017.

Warneke, C., de Gouw, J. A., Holloway, J. S., Peischl, J., Ryerson, T. B., Atlas, E., Blake, D., Trainer, M., and Parrish, D. D.: Multiyear trends in volatile organic compounds in Los Angeles, California: five decades of decreasing emissions, J. Geophys. Res. Atmos., 117(17), 1-10, https://doi.org/10.1029/2012JD017899, 2012.

Wei, X. Y., Liu, M., Yang, J., Du, W. N., Sun, X., Huang, Y. P., Zhang, X., Khalil, S. K., Luo, D. M., and Zhou, Y. D.: Characterization of $PM_{2.5}$-bound PAHs and carbonaceous aerosols during three-month severe haze episode in Shanghai, China: Chemical composition, source approtionment and long-range transportation, Atmos. Environ., 203, 1-9, https://doi.org/10.1016/j.atmosenv.2019.01.046, 2019.

Wongphatarakul, V., Fridelander, S. K., and Pinto, J. P.: A comparative study of $PM_{2.5}$ ambient aerosol chemical databases, Environ. Sci. Technol., 32, 3926-3934, https://doi.org/10.1016/S0021-8502(98)00164-5, 1998.

Wu, R. R., Li, J., Hao, Y. F., Li, Y. Q., Zeng, L. M., and Xie, S. D.: Evolution process and sources of ambient volatile organic compounds during a severe haze event in Beijing, China, Sci. Total Environ., 560-561, 62-72, https://doi.org/10.1016/j.scitotenv.2016.04.030, 2016.

Xie, Y. L., and Berkowitz, C. M.: The use of conditional probability functions and potential source contribution functions to identify source regions and advection pathways of hydrocarbon emissions in Houston, Texas, Atmos. Environ., 41, 5831-5847, https://doi.org/10.1016/j.atmosenv.2007.03.049, 2007.

Xiong, Y., and Du, K.: Source-resolved attribution of ground-level ozone formation potential from VOC emissions in Metropolitan Vancouver, BC, Sci. Total Environ., 721, 137698, https://doi.org/10.1016/j.scitotenv.2020.137698, 2020.

Xu, J. M., Tie, X. X., Gao, W., Lin, Y. F., Fu, and Fu, Q. Y.: Measurement and model analyses of the ozone variation during 2006 to 2015 and its response to emission change in megacity Shanghai, China, Atmos. Chem. Phys. 19, 9017-9035, https://doi.org/10.5194/acp-19-9017-2019, 2019.

Yan, Y. L., Peng, L., Li, R. M., Li, Y. H., Li, L. J., and Bai, H. L.: Concentration, ozone formation potential and source analysis of volatile organic compounds (VOCs) in a thermal power station centralized area: A study in Shuozhou, China, Environ. Pollut., 223, 295-304, https://doi.org/10.1016/j.envpol.2017.01.026, 2017.

Yao, Z., Wu, B., Shen, X., Cao, X., Jiang, X., Ye, Y., and He, K.: On-road emission characteristics of VOCs from rural vehicles and their ozone formation potential in Beijing, China, Atmos. Environ., 105, 91-96, https://doi.org/10.1016/j.atmosenv.2015.01.054, 2015.

Yang, K. J., Kong, L. D., Tong, S. Y., Shen, J. D., Chen, L., Jin, S. Y., Wang, C., Sha, F., and Wang, L.: Double High-Level Ozone and $PM_{2.5}$ Co-Pollution Episodes in Shanghai, China: Pollution Characteristics and Significant Role of Daytime HONO, 12, 5, https://doi.org/10.3390/atmos12050557, 2021.

Yang, M. R., Li, F. X., Huang, C. Y., Tong, L., Dai, X. R., and Xiao, H.: VOC characteristics and their source apportionment in a coastal industrial area in the Yangtze River Delta, China, J. Environ. Sci., 127, 483-493, https://doi.org/10.1016/j.jes.2022.05.041, 2023.

Yang, Y. R., Liu, X. G., Qu, Y., An, J. L., Jiang, R., and Zhang, Y. H.: Characteristics and formation mechanism of continuous hazes in China: a case study during the autumn of 2014 in the North China Plain, Atmos. Chem. Phys., 15, 8165-8178, https://doi.org/10.5194/acpd-15- 10987-2015, 2015.

Yoo, J. M., Jeong, M. J., Kim, D., Stockwell, W. R., Yang, J. H., Shin, H. W., Lee, M. I., Song, C. K., and Lee, S. D.: Spatiotemporal variations of air pollutants (O_3, NO_2, SO_2, CO, PM_{10}, and VOCs) with land-use types, Atmos. Chem. Phys., 15, 10857-10885, https://doi.org/10.5194/acp-15-10857-2015, 2015.

Yu, S. J., Su, F. C., Yin, S. S., Wang, S. B., Xu, R. X., He, B., Fan, X. G., Yuan, M. H., and Zhang, R. Q.: Characterization of ambient volatile organic compounds, source apportionment, and the ozone-NOx-VOC sensitivities in a heavily

polluted megacity of central China: Effect of sporting events and the emission reductions, Atmos. Chem. Phys., 293, 1-61, https://doi.org/10.5194/acp-21-15239-2021, 2021.

Yuan, B., Hu, W. W., Shao, M., Wang, M., Chen, W. T., Lu, S. H., Zeng, L. M., and Hu, M.: VOCs emissions, evolutions and contributions to SOA formation at a receptor site in eastern China, Atmos. Chem. Phys., 13(17), 8815-8832, https://doi.org/10.5194/acp-13-8815-2013, 2013.

Yuan, B., Shao, M., Lu, S., and Wang, B.: Source profiles of volatile organic compounds associated with solvent use in Beijing, China, Atmos. Environ., 44, 1919-1926, https://doi.org/10.1016/j.atmosenv.2010.02.014, 2010.

Yuan, B., Hu, W. W., Shao, M., Wang, M., Chen, W. T., Lu, S. H., Zeng, L. M., and Hu, M.: VOCs emissions, evolutions and contributions to SOA formation at a receptor site in eastern China, Atmos. Chem. Phys., 13(17), 8815-8832, https://doi.org/10.5194/acp-13-8815-2013, 2013.

Zhan, J. L., Feng, Z. M., Liu, P. F., He, X. W., He, Z. M., Chen, T. Z., Wang, Y. F., He, H., Mu, Y. J., and Liu, Y. C.: Ozone and SOA formation potential based on photochemical loss of VOCs during the Beijing summer, Environ. Pollut., 285, 117444, https://doi.org/10.1016/j.envpol.2021.117444, 2021.

Zhang, D., He, B., Yuan, M. H., Yu, S. J., Yin, S. S., and Zhang, R. Q.: Characteristics, sources and health risks assessment of VOCs in Zhengzhou, China during the haze pollution season, J. Environ. Sci., 108, 44-57, https://doi.org/10.1016/j.jes.2021.01.035, 2021.

Zhang, F., Shang, X. N., Chen, H., Xie, G. Z., Fu, Y., Wu, D., Sun, W. W., Liu, P. F., Wang, G. H., and Chen, J. M.: Significant impact of coal combustion on VOCs emissions in winter in a North China rural site, Sci. Total Environ., 720, 137617, 1-11, https://doi.org/10.1016/j.scitotenv.2020.137617, 2020b.

Zhang, G., Wang, N., Jiang, X., and Zhao, Y.: Characterization of ambient volatile organic compounds (VOCs) in the area adjacent to a petroleum refinery in Jinan, China, Aerosol Air Qual. Res., 17(4), 944-950, https://doi.org/10.4209/aaqr.2016.07.0303, 2017.

Zhang, K., Li, L., Huang, L., Wang, Y. J., Huo, J. T., Duan, Y. S., Wang, Y. H., and Fu, Q. Y.: The impact of volatile organic compounds on ozone formation in the suburban area of Shanghai, Atmos. Environ., 232(137617), 1-11, https://doi.org/10.1016/j.atmosenv.2020.117511, 2020a.

Zhang, S. B., Wang, S. S., Zhang, R. F., Guo, Y. L., Yan, Y. H., Ding, Z. F., and Zhou, B.: Investigating the Sources of Formaldehyde and Corresponding Photochemical Indications at a Suburb Site in Shanghai From MAX-DOAS Measurements, 126, 6, J. Geophys. Res-Atmos., https://doi.org/10.1029/2020JD033351, 2021.

Zhang, Y., Wang, X., Zhang, Z., Lu, S., Shao, M., Lee, F. S. C., and Yu, J.: Species profiles and normalized reactivity of volatile organic compounds from gasoline evaporation in China, Atmos. Environ., 79, 110-118, https://doi.org/10.1016/j.atmosenv.2013.06.029, 2013.

Zhang, Y. C., Li R., Fu H. B., Zhou D., and Chen J. M.: Observation and analysis of atmospheric volatile organic compounds in a typical petrochemical area in Yangtze River Delta, China, J. Environ. Sci., 71, 233-248, https://doi.org/CNKI:SUN:HJKB.0.2018-09-022, 2018.

Zheng, J., Yu, Y., Mo, Z., Zhang, Z., Wang, X., Yin, S., Peng, K., Yang, Y., Feng, X., and Cai, H.: Industrial sector-based volatile organic compound (VOC) source profiles measured in manufacturing facilities in the Pearl River Delta, China, Sci. Total Environ., 456, 127-136, https://doi.org/10.1016/j.scitotenv.2013.03.055, 2013.

Zheng, J. Y., Zhong, L. J., Wang, T., Louie, P. K. K., and Li, Z. C.: Ground-level ozone in the Pearl River Delta region: analysis of data from a recently established regional air quality monitoring network, Atmos. Environ., 44, 814-823, https://doi.org/10.1016/j.atmosenv.2009.11.032, 2010.

Zheng, H., Kong, S. F., Xing, X. L., Mao, Y. , Hu, Y. P., Ding, Y., Li, G., Liu, D. T., Li, S. L., and Qi, S. H.: Monitoring of volatile organic compounds (VOCs) from an oil and gas station in northwest China for 1 year, Atmos. Chem. Phys., 18(7), 4567-4595, https://doi.org/10.5194/acp-2017-828, 2018.

Zheng, H., Kong, S. F., Yan, Y. Y., Chen, N., Yao, L. Q., Liu, X., Wu, F. Q., Cheng, Y., Niu, Z. Z., Zheng, S. R., Zeng, X., Yan, Q., Wu, J., Zheng, M. M., Liu, D. T., Zhao, D. L., and Qi, S. H.: Compositions, sources and health risks of ambient volatile organic compounds (VOCs) at a petrochemical industrial park along the Yangtze River, Sci. Total. Environ., 73, 135505, 1-12, https://doi.org/10.1016/j.scitotenv.2019.135505, 2020.

Zhu, H. L., Wang, H. L., Jing, S. G., Wang, Y. F., Cheng, T. T., Tao, S. K., Lou, S. R., Qiao, L. P., Li, L., and Chen, J. M.: Characteristics and sources of atmospheric volatile organic compounds (VOCs) along the mid-lower Yangtze River in China, Atmos. Environ., 190(7), 232-240, https://doi.org/10.1016/j.atmosenv.2018.07.026, 2018.

Zhu, Y., Yang, L., Chen, J., Wang, X., Xue, L., Sui, X., Wen, L., Xu, C., Yao, L., Zhang, J., Shao, M., Lu, S., and Wang, W.: Characteristics of ambient volatile organic compounds and the influence of biomass burning at a rural site in Northern China during summer 2013, Atmospheric Environment, 124, 156-165, https://doi.org/10.1016/j.atmosenv.2015.08.097, 2016.

Zhu, Y. H., Yang, L. X., Kawamura, K., Chen, J. M., Ono, K. R., Wang, X. F., Xue, L. K., and Wang, W. X.: Contribution and source identification of biogenic and anthropogenic hydrocarbons to secondary organic aerosols at Mt. Tai in 2014, Environ. Pollut., 220, 863-872, https://doi.org/10.1016/j.envpol.2016.10.070, 2017.

Zou, B. B., Huang, X. F., Zhang, B., Dai, J., Zeng, L. W., Feng, N., and He, L. Y.: Source apportionment of $PM_{2.5}$ pollution in an industrial city in southern China, Atmos. Pollut. Re., 8(6), 1193-1202, https://doi.org/10.1016/j.apr.2017.05.001, 2017.
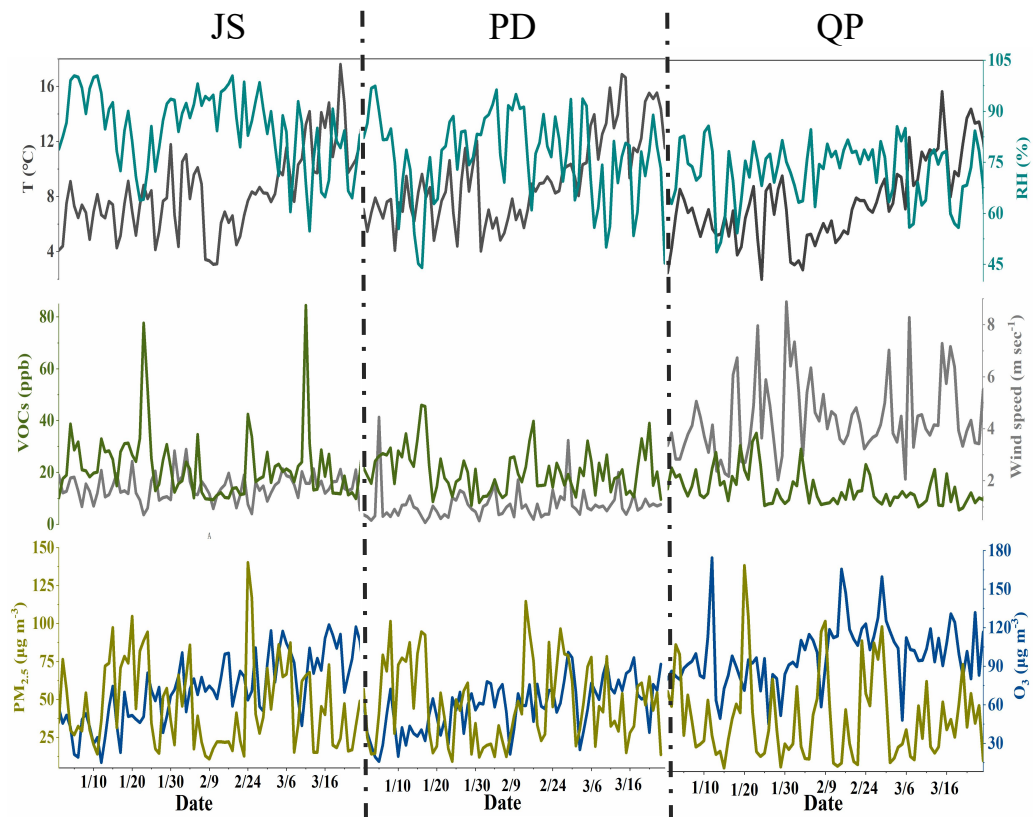
Figure 1: Time series of temperature (T), relative humidity (RH), wind speed, VOC categories, PM$_{2.5}$ and O$_3$ at the (a) JS, (b) PD and (c) QP sites.
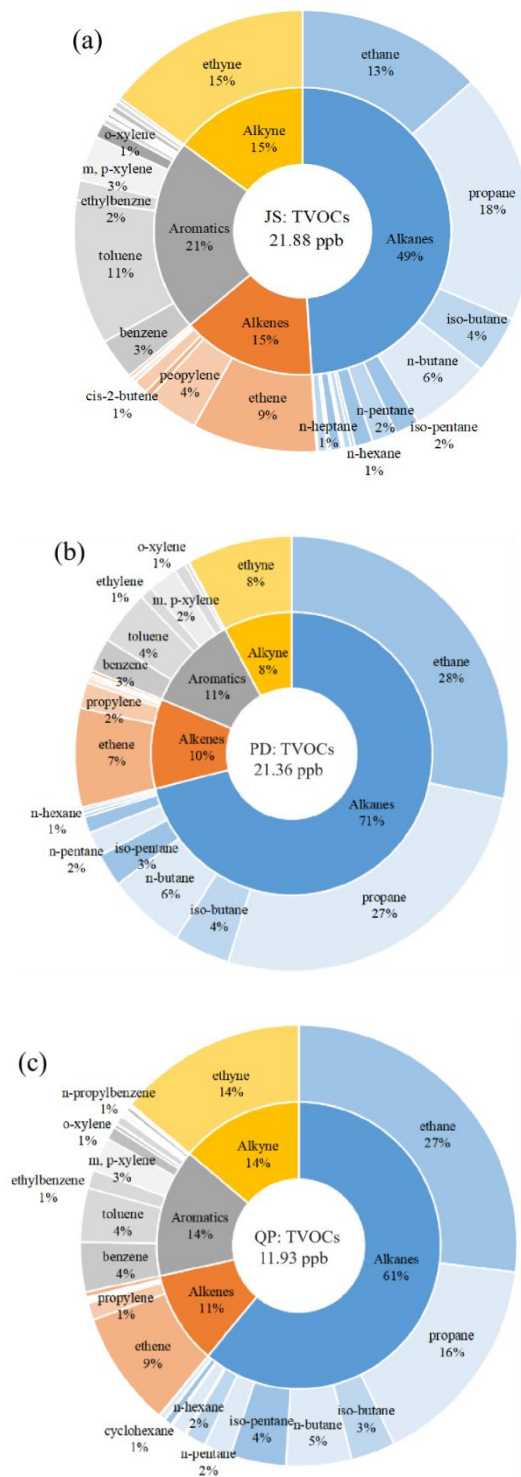
Figure 2: Contributions of the VOC categories (43 species) at the (a) JS, (b) PD and (c) QP sites (the contributions > 1 % were marked).
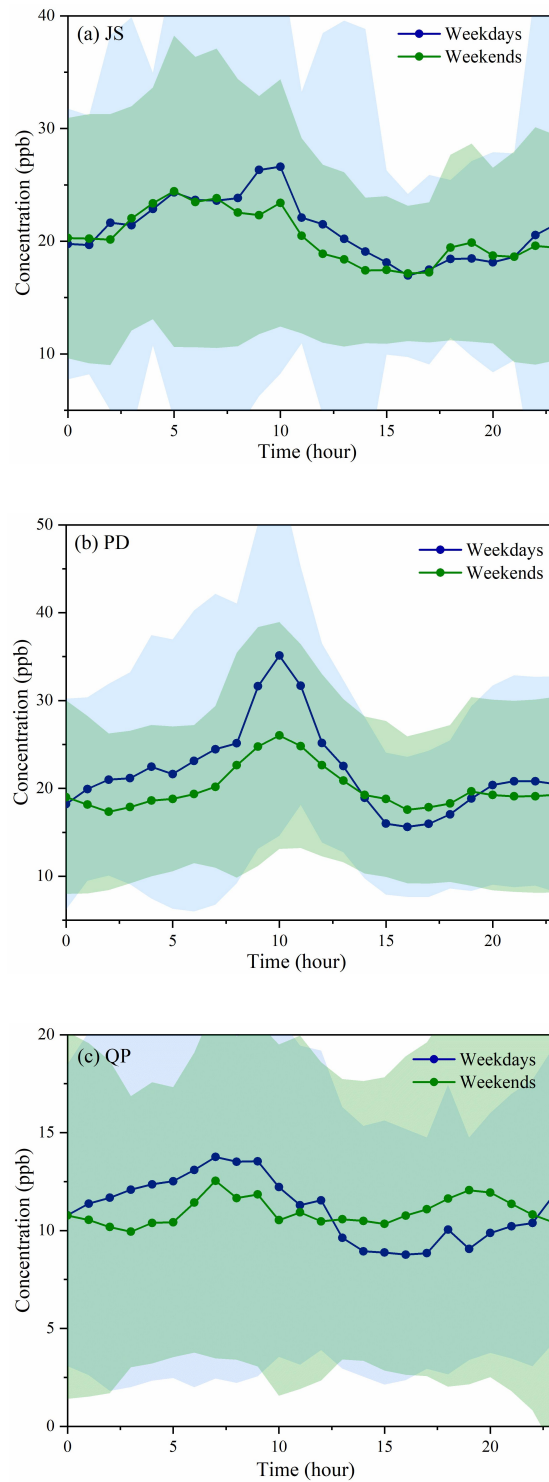
Figure 3: "Weekend effects" of the TVOC concentrations at the sampling sites.
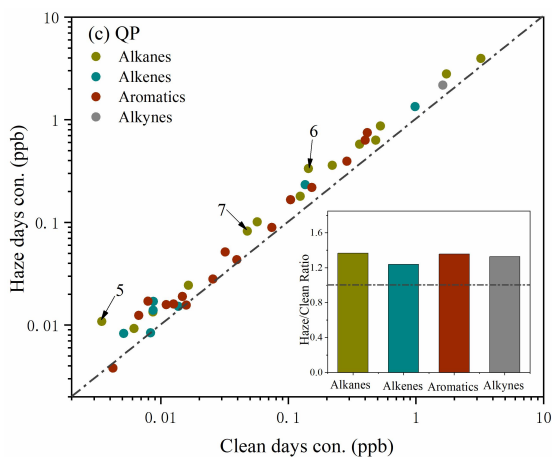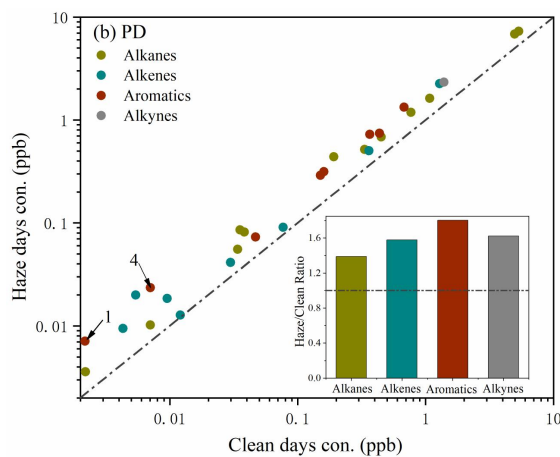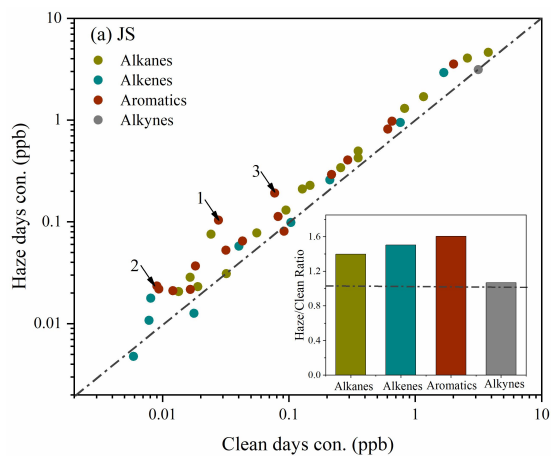
Figure 4: Differences in the VOC concentrations between the clean and haze days at the (a) JS, (b) PD and (c) QP sites. 1: 1, 2, 4-trimethylbenzene; 2: *p*-ethyltoluene; 3: *m*-ethyltoluene; 4: ethylbenzene; 5: 2, 2, 4-trimethylpentane; 6: *n*-hexane; 7: *h*-heptane.
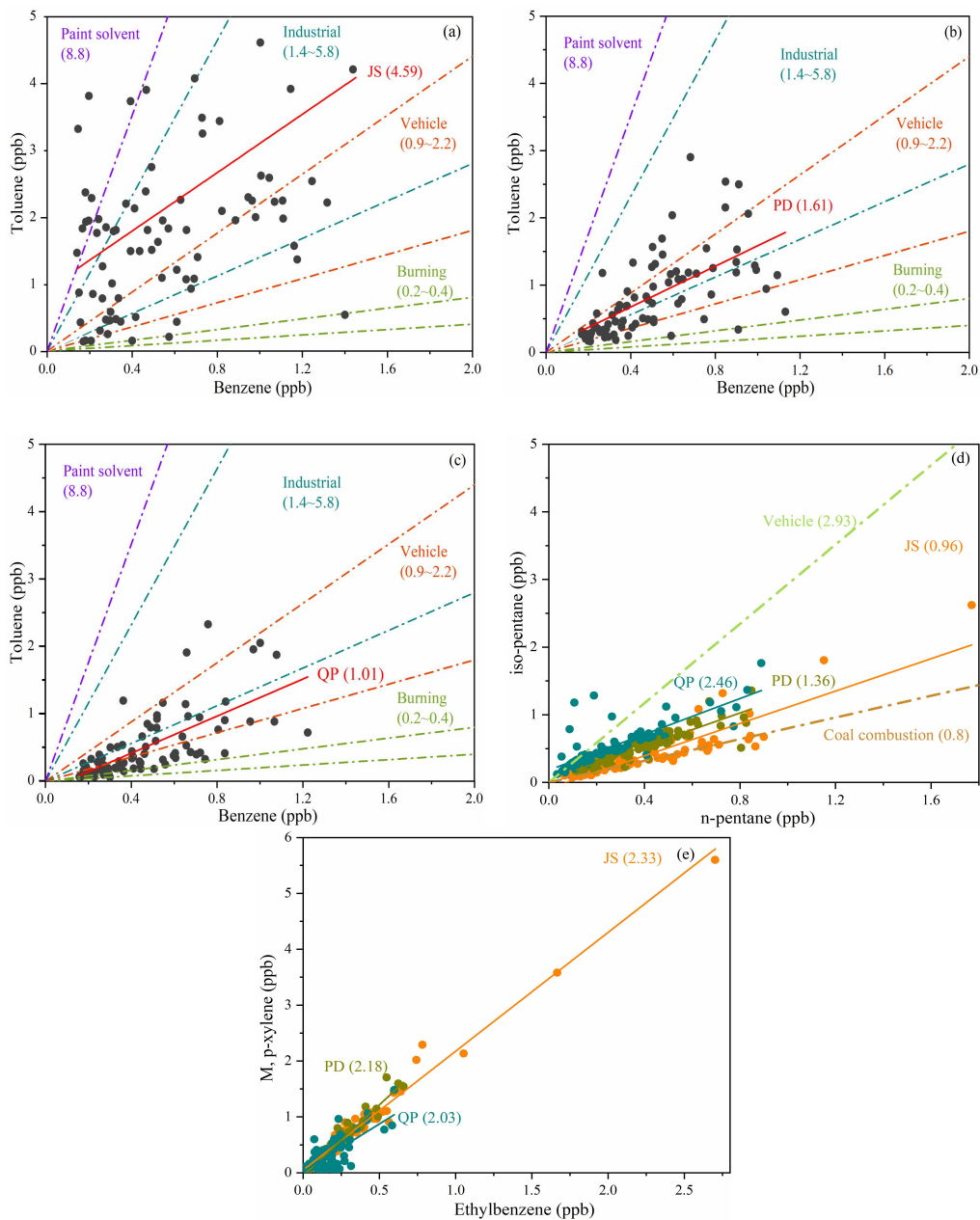
Figure 5: Specific ratios of the target VOC species for the source identification. The linear correlations between toluene and benzene at the (a) JS, (b) PD and (c) QP sites, and (d) *m, p*-xylene and ethylbenzene and (e) *iso*-pentane and *n*-pentane at JS (orange), PD (yellow) and QP (blue).

a. JS

b. PD
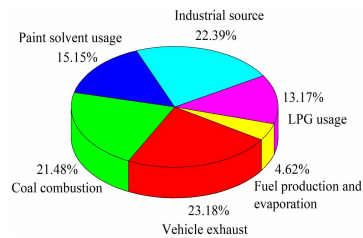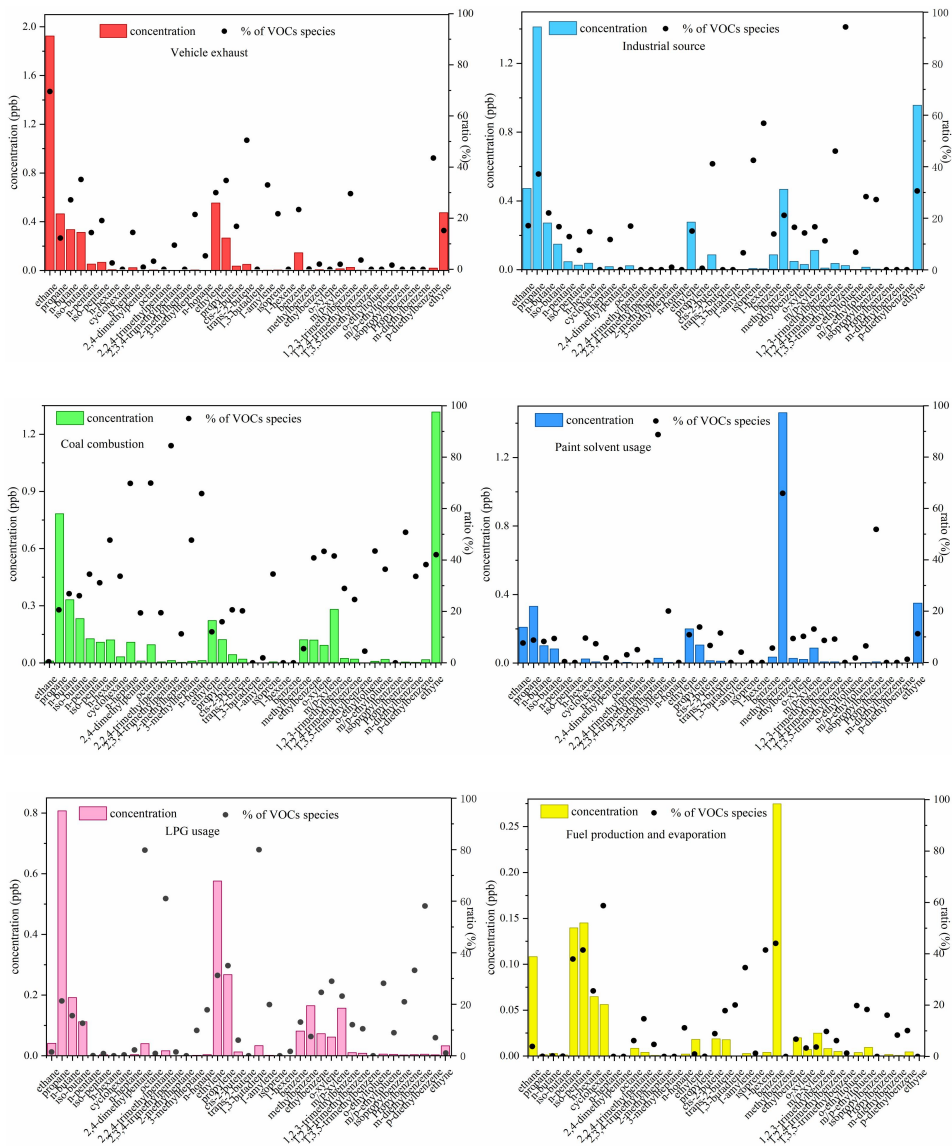
c. QP
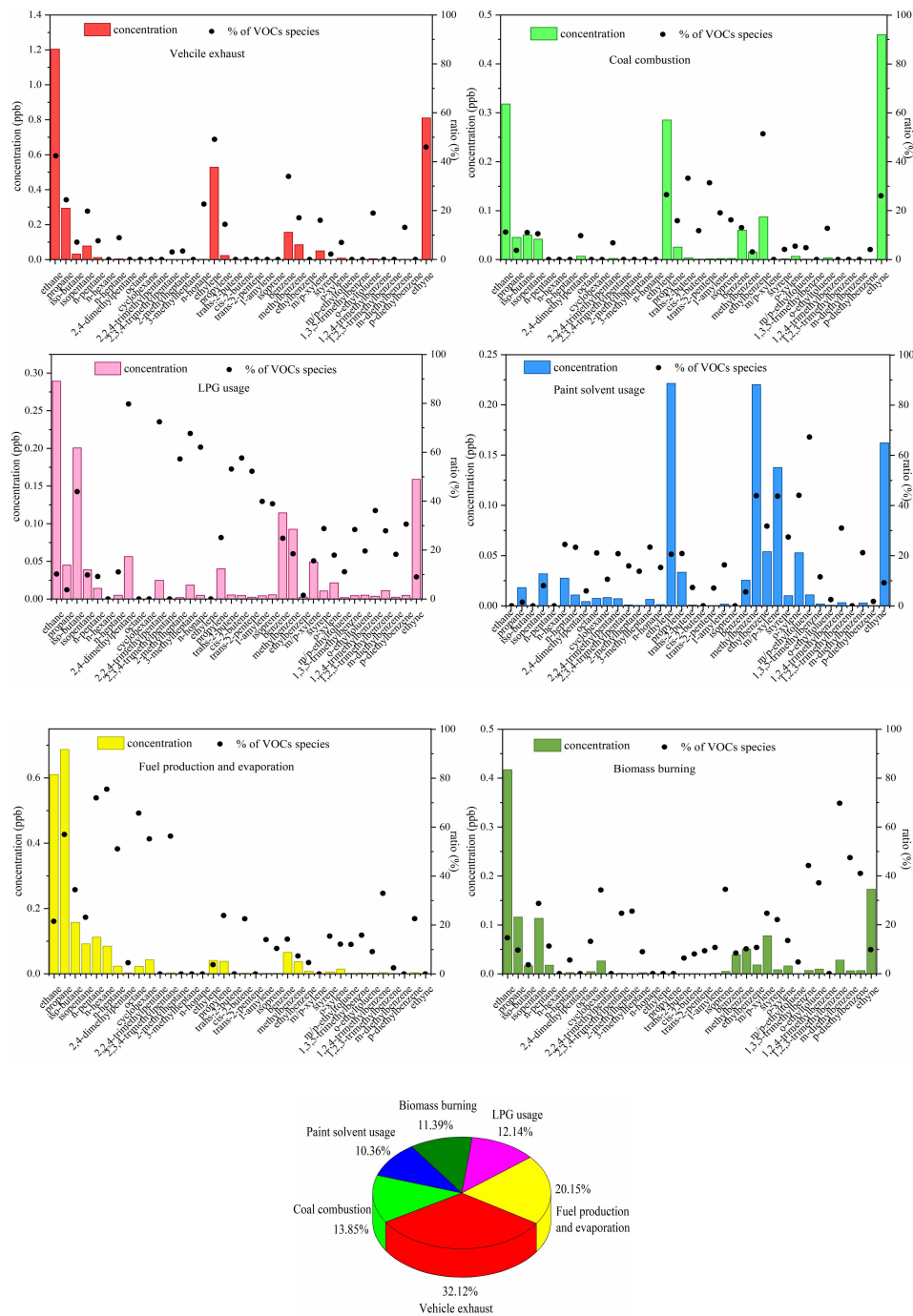
Figure 6: Sources profiles and contributions of VOCs at the (a) JS, (b) PD and (c) QP sites.
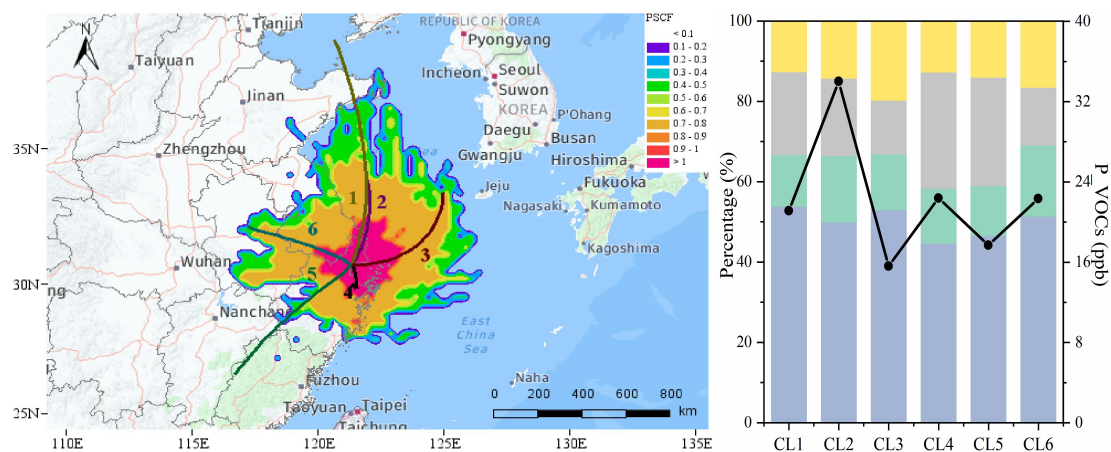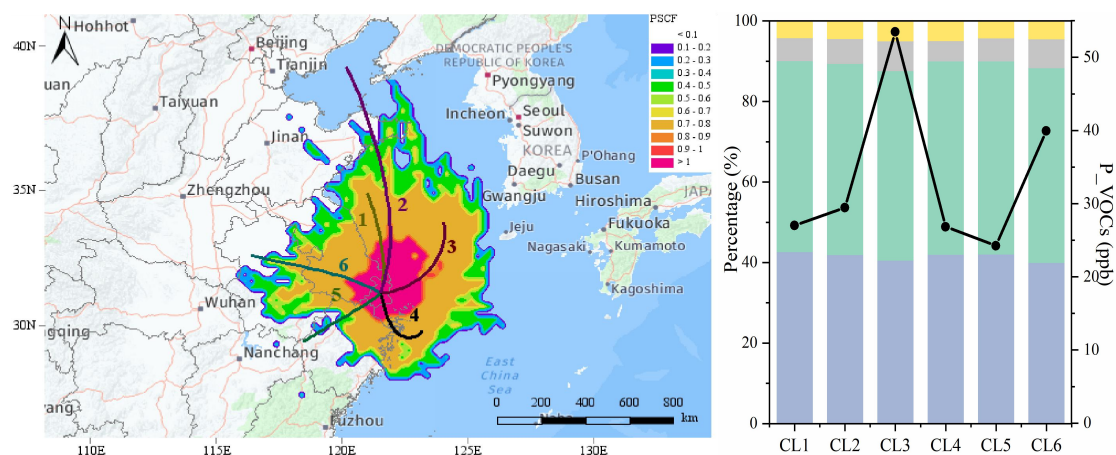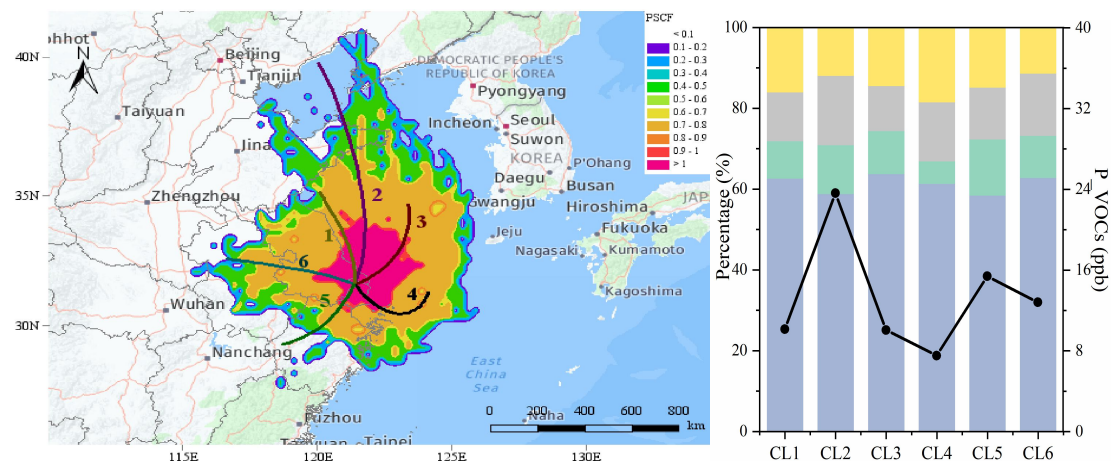
Figure 7: Backward trajectory cluster analysis (24 h) and PSCF analysis at the JS, PD and QP sites.
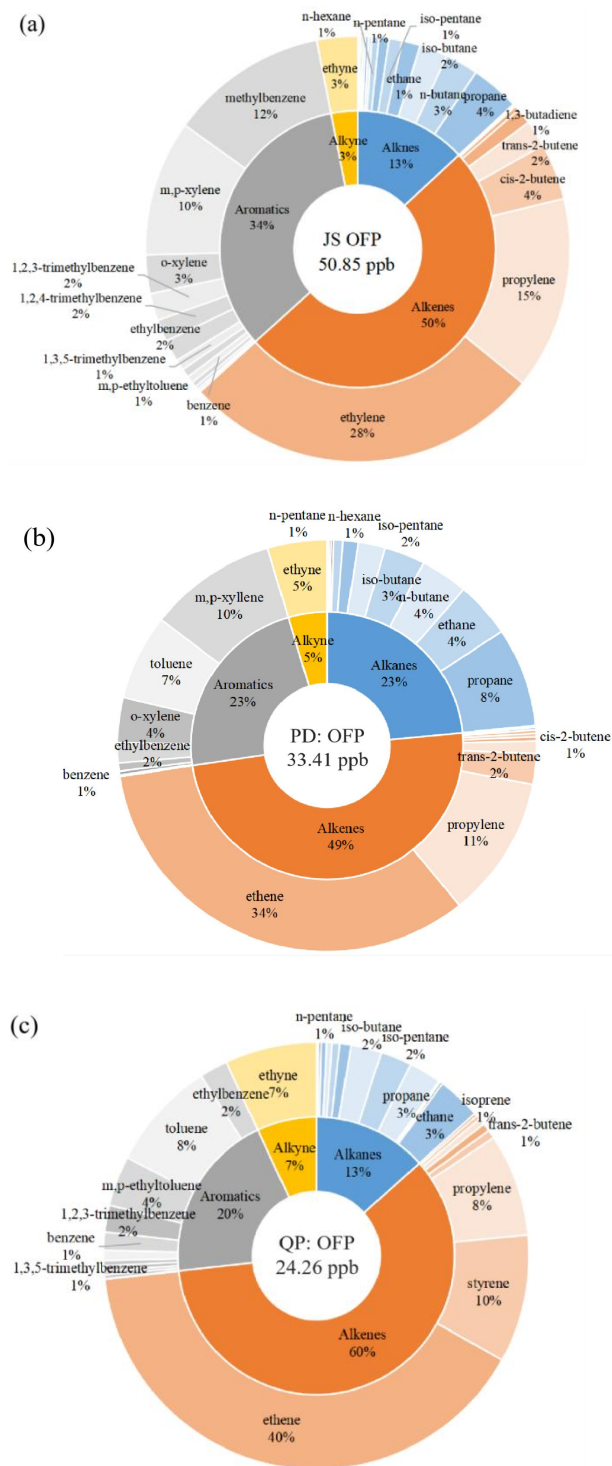
Figure 8: Contributions of VOCs to OFP at the (a) JS, (b) PD and (c) QP sites (the contributions > 1 % were marked).
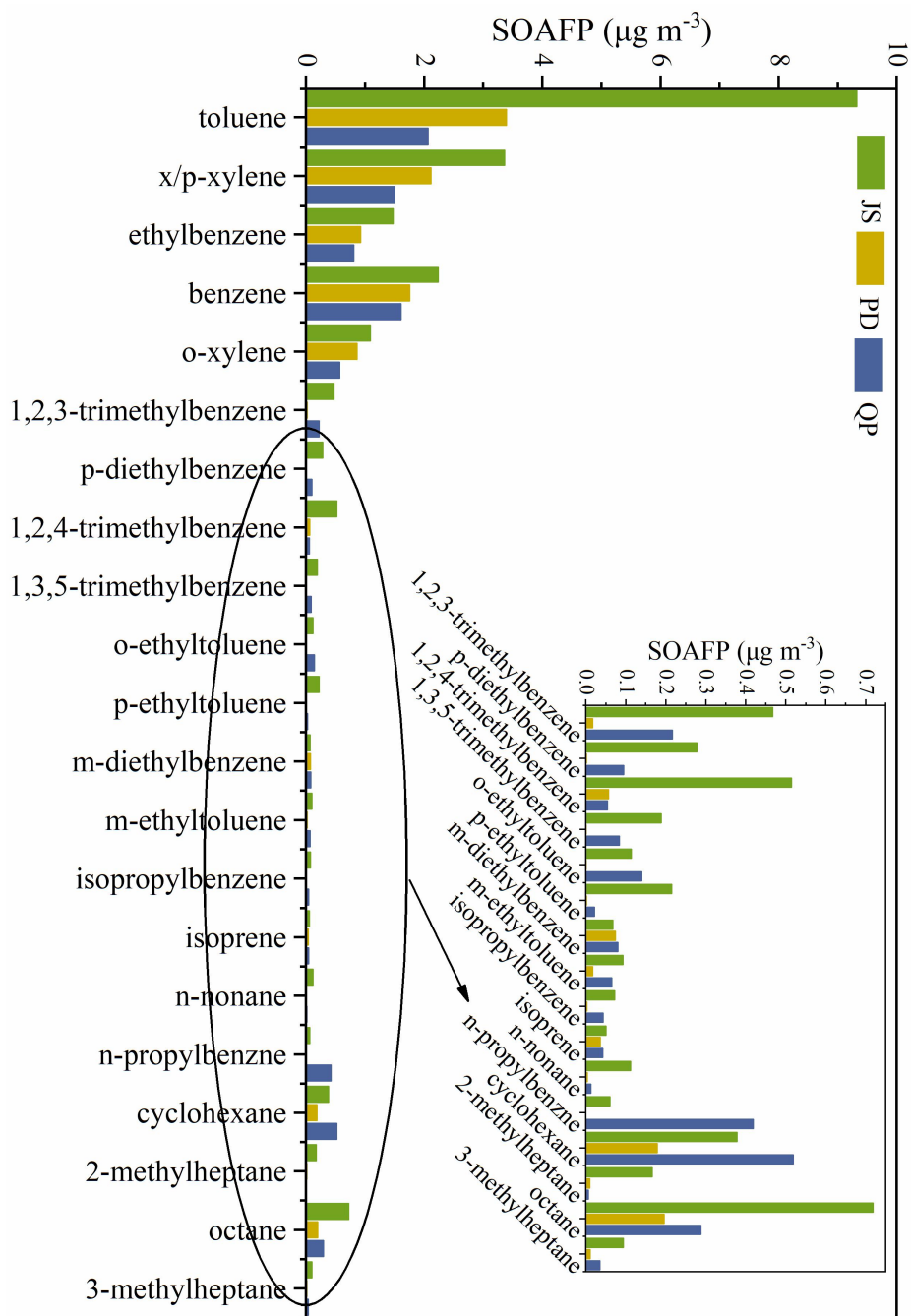
Figure 9: The SOAFP analysis of different VOC species at the JS, PD and QP sites.
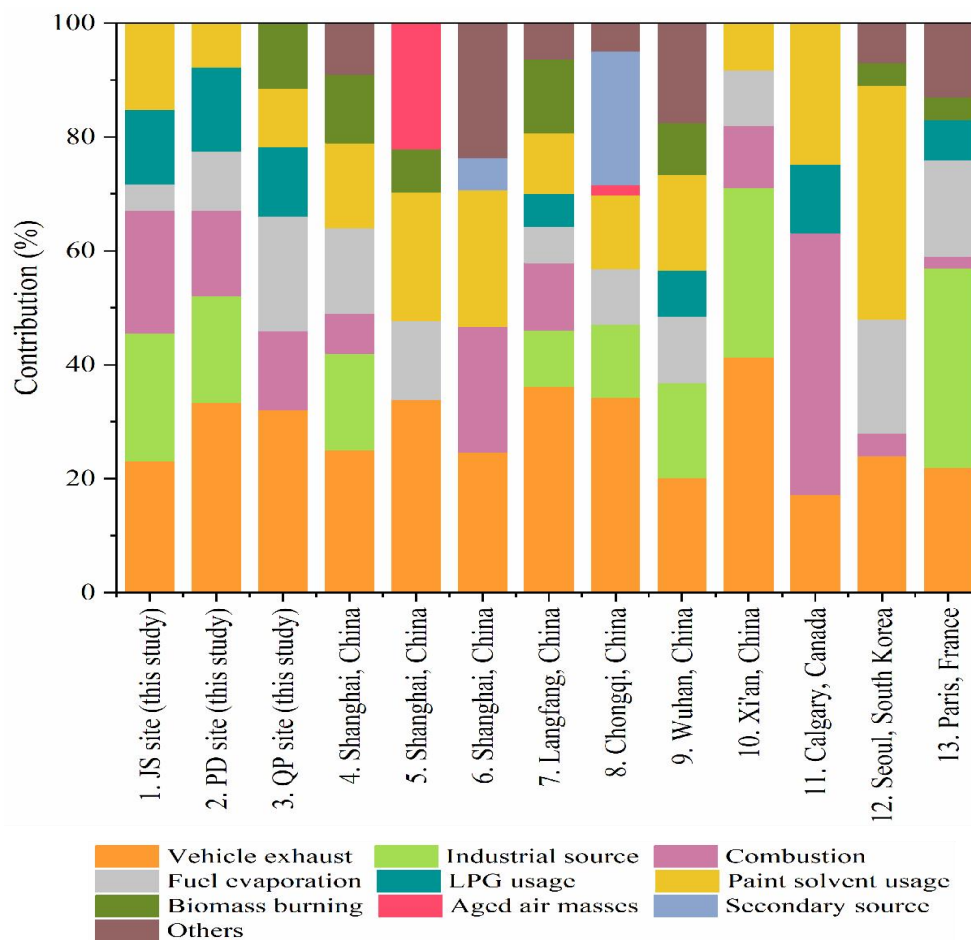
Figure 10: Primary emissions of the observed atmospheric VOCs of this study, and those measured at different locations or during different periods: 1, 2, 3. Shanghai, China (this study); 4. Shanghai, China (Cai et al., 2010a); 5. Shanghai, China (Liu et al., 2019); 6. Shanghai, China (Liu et al., 2021); 7. Langfang, China (Song et al., 2019a); 8. Chongqi, China (Li et al., 2018); 9. Wuhan, China (Hui et al., 2018); 10. Xi'an, China (Song et al., 2021); 11. Calgary, Canada (Bari and Kindzierski, 2018); 12. Seoul, South Lorea (Song et al., 2019b); 13. Paris, France (Gaimoz et al., 2011)
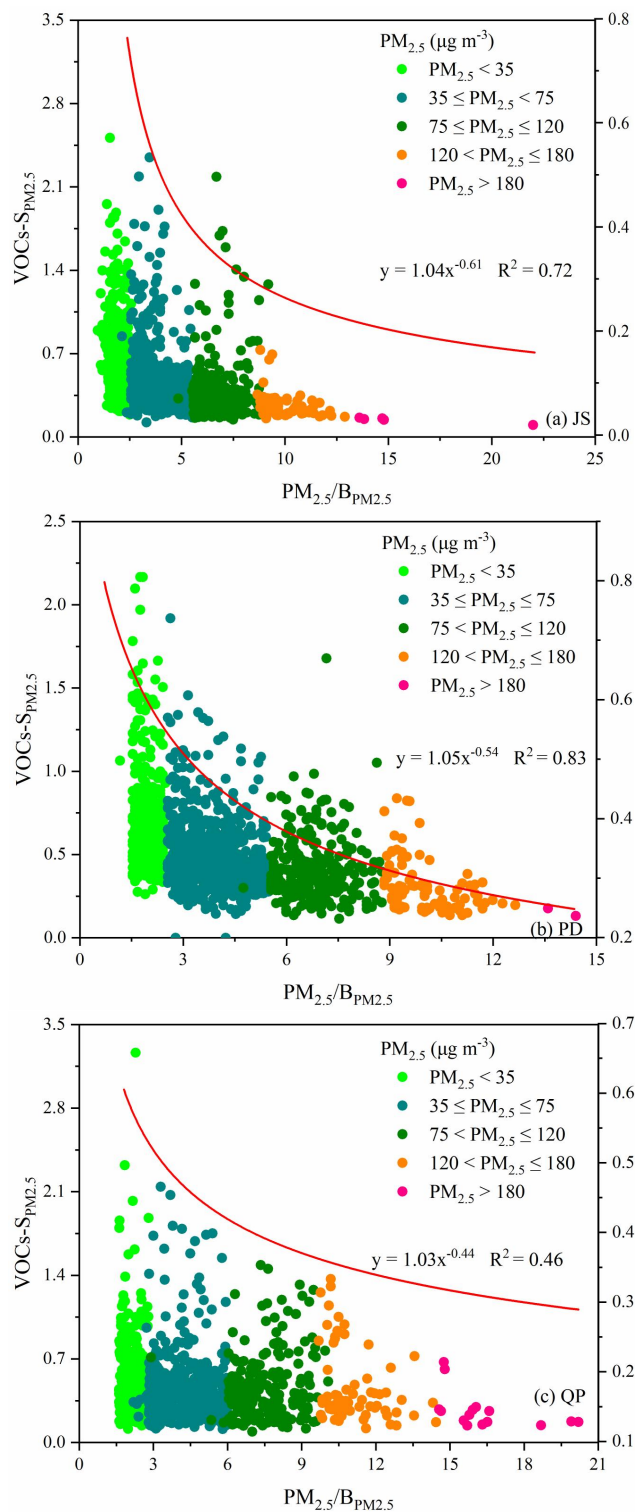
Figure 11: The variations of VOCs-S$_{PM2.5}$ at the different level of PM$_{2.5}$ at the JS, PD and QP sites.

Table 1: Air mass cluster trajectories at the JS, PD and QP sites.

Site	Cluster	Ratio (%)	P_Ratio (%)	P_TVOCs (ppb)
JS	1	16.67	28.04	21.13
	2	29.07	18.03	34.03
	3	19.46	16.62	15.62
	4	12.26	12.75	22.40
	5	5.92	16.62	17.70
	6	16.62	5.93	22.34
PD	1	18.04	33.13	27.03
	2	17.80	10.42	29.45
	3	34.19	21.59	53.48
	4	8.57	15.28	26.85
	5	10.84	8.53	24.25
	6	10.56	11.04	39.95
QP	1	14.20	18.47	10.15
	2	17.57	13.50	23.63
	3	31.87	27.81	10.07
	4	15.20	16.79	7.53
	5	8.71	14.52	15.39
	6	12.45	8.91	12.81